Power and bandwidth allocation in multibeam satellite systems

Author

Aleix París i Bordas

Supervisors

Prof. Edward F. Crawley

Dr. Bruce G. Cameron

System Architecture Lab

Department of Aeronautics and Astronautics

Massachusetts Institute of Technology

June 2018

Abstract

Communications satellites are becoming more flexible and complex. New generations feature on-board signal processing and provide hundreds of Gbit/s of throughput. Therefore, dynamic resource management (DRM) is increasingly becoming one of the challenges faced today by satellite operators.

In recent years there has been considerable interest in DRM for communications satellites. Previous studies have proposed power allocation to beams using genetic algorithms and joint power and bandwidth allocation using analytical approaches as well as the Lagrange multipliers technique. Nevertheless, there is a research gap in metaheuristics/artificial intelligence algorithms in communications satellites to allocate both power and bandwidth while considering important factors such as the interference between beams. Therefore, this thesis aims to develop a new methodology of power and bandwidth allocation in multibeam satellite systems taking into account interferences and to investigate the improvement of dynamically allocating bandwidth in addition to power.

First, the model is explained and results on simple case studies are shown in order to analyze how power and bandwidth influence the data rate in communications satellites. Then, the proposed algorithm is explained and the outcomes from simulations are presented. Results indicate that apart from allocating power, the unmet system capacity (USC) can be further reduced by allocating bandwidths per beam. The genetic algorithm implemented in this thesis can diminish the USC in 10% - 15%. Furthermore, the demand variation has an effect on that improvement: the higher this variation is, the more important it is to allocate also bandwidths and to allow them a higher flexibility in order to obtain the best solution (and vice versa).

Resum

Els satèl·lits de comunicacions són cada vegada més flexibles i complexos. Les noves generacions tenen processament de senyals a bord i proporcionen taxes de bits de centenars de Gbit/s. Per tant, la gestió dinàmica de recursos (DRM en anglès) s'està convertint cada cop més en un dels desafiaments als quals s'enfronten els operadors de satèl·lits.

En els últims anys hi ha hagut un considerable interès en DRM per a satèl·lits de comunicacions. Estudis previs han proposat l'assignació de potència a feixos utilitzant algorismes genètics i l'assignació conjunta de potència i amplada de banda utilitzant enfocaments analítics, així com la tècnica de multiplicadors de Lagrange. No obstant això, hi ha una escassetat de recerca en algorismes metaheurístics o d'intel·ligència artificial en satèl·lits de comunicacions per assignar tant la potència com l'amplada de banda que a més considerin factors importants com la interferència entre feixos. Per tant, aquesta tesi pretén desenvolupar una nova metodologia d'assignació de potència i amplada de banda en sistemes de satèl·lits multifeix tenint en compte interferències i investigar la millora de l'assignació dinàmica de l'amplada de banda a més de la potència.

En primer lloc s'explica el model i es mostren els resultats de casos d'estudi simples per analitzar com la potència i l'amplada de banda influeixen en la velocitat de dades en satèl·lits de comunicacions. Posteriorment s'explica l'algorisme proposat i es presenten els resultats de les simulacions. Els resultats indiquen que, a més d'assignant potència, la capacitat del sistema no satisfeta (USC en anglès) es pot reduir encara més mitjançant l'assignació d'amplades de banda per feix. L'algorisme genètic implementat en aquesta tesi pot disminuir la USC en 10 % - 15 %. A més, la variació de la demanda té un efecte en aquesta millora: com més alta és, més important és assignar també amplades de banda i permetre'ls una major flexibilitat per obtenir la millor solució (i viceversa).

Resumen

Los satélites de comunicaciones son cada vez más flexibles y complejos. Las nuevas generaciones cuentan con procesamiento de señales a bordo y proporcionan tasas de bits de cientos de Gbit/s. Por lo tanto, la gestión dinámica de recursos (DRM en inglés) se está convirtiendo en mayor medida en uno de los desafíos a los que se enfrentan los operadores de satélites.

En los últimos años ha habido un considerable interés en DRM para satélites de comunicaciones. Estudios previos han propuesto la asignación de potencia a haces utilizando algoritmos genéticos y la asignación conjunta de potencia y ancho de banda utilizando enfoques analíticos, así como la técnica de multiplicadores de Lagrange. Sin embargo, existe una escasez de investigación en algoritmos metaheurísticos o de inteligencia artificial en satélites de comunicaciones para asignar tanto la potencia como el ancho de banda que además consideren factores importantes como la interferencia entre haces. Por lo tanto, esta tesis pretende desarrollar una nueva metodología de asignación de potencia y ancho de banda en sistemas de satélites multihaz teniendo en cuenta interferencias e investigar la mejora de la asignación dinámica del ancho de banda además de la potencia.

En primer lugar se explica el modelo y se muestran los resultados de casos de estudio simples para analizar cómo la potencia y el ancho de banda influyen en la velocidad de datos en satélites de comunicaciones. Posteriormente se explica el algoritmo propuesto y se presentan los resultados de las simulaciones. Los resultados indican que, además de asignando potencia, la capacidad del sistema no satisfecha (USC en inglés) se puede reducir aún más mediante la asignación de anchos de banda por haz. El algoritmo genético implementado en esta tesis puede disminuir la USC en 10 % - 15 %. Además, la variación de la demanda tiene un efecto en esa mejora: cuanto más alta es, más importante es asignar también anchos de banda y permitirles una mayor flexibilidad para obtener la mejor solución (y viceversa).

Acknowledgments

First and foremost, I would like to truly thank Prof. Edward Crawley and Dr. Bruce Cameron for their invaluable support and for supervising this thesis throughout my stay at MIT. It has been a pleasure and an honor to work with you.

I would also like to thank Íñigo del Portillo for his generous help and advice during hard times, and for sharing his extensive experience in communications satellites and Python with me. This thesis could not have been done without your input.

Thank you Axel, Juanjo, Nikko, Florian, Anne, Veronica, Matthew, Andrew, Alejandro, George and Johannes from the 33-409 office. You helped creating a welcoming environment during my stay and have been a source of inspiration. I would like to especially thank Íñigo (again) and Markus for their help reviewing this thesis.

This extraordinary opportunity, a research stay at MIT, would not have been possible without the intervention and economic help from the Centre de Formació Interdisciplinària Superior, CFIS. I am also grateful to this center for coordinating the Aerospace Engineering and Computer Science syllabus I followed at UPC – BarcelonaTech.

My stay in Boston has been as best as possible thanks to Adrià, Albert, Esteve, Maria, Martí, Miquel and Oleguer, to name a few. We shared so many fun experiences that helped me disconnect and made me feel like home.

Last but not least, I would like to express my gratitude for the unconditional support given to me by my father Jordi and my brother Gerard, and for always believing in me. I would not be who I am today without their help.

Contents

List of Figures

List of Tables

Chapter 1

Introduction

1.1 Motivation

The space economy is experimenting an accelerated growth due to technological advancements. Revenues were \$329M in 2016, and they are expected to be \$1.1T in 2040 [1]. In particular, the satellite communications market is growing fast, and has changed significantly in the last 30 years [2] because of an increased demand of connectivity services to remote locations that do not have ground communications infrastructures [3] or to serve the mobility sector (airplanes and ships).

To deal with this rising demand, satellite operators are transitioning towards more flexible satellites [4]; recent satellite designs are replacing analogue payloads with digital communication payloads which will allow for more flexible resource allocation [1]. Whereas older generations of satellites had a bent-pipe architecture (the uplink signal was relayed back to Earth through a particular beam after being amplified and shifted in frequency), new satellites provide advanced adaptability (dynamic power and bandwidth allocations, routing capabilities, etc). In addition, these "regenerative" satellites are able to demodulate and decode the signal in order to encode and modulate it again after applying error detection and correction techniques. Figure 1-1 exposes technologies that different generations of satellites implement, depicting the shift from the old bent-pipe to the regenerative satellites.

Another technology that has significantly increased the capacity of modern com-
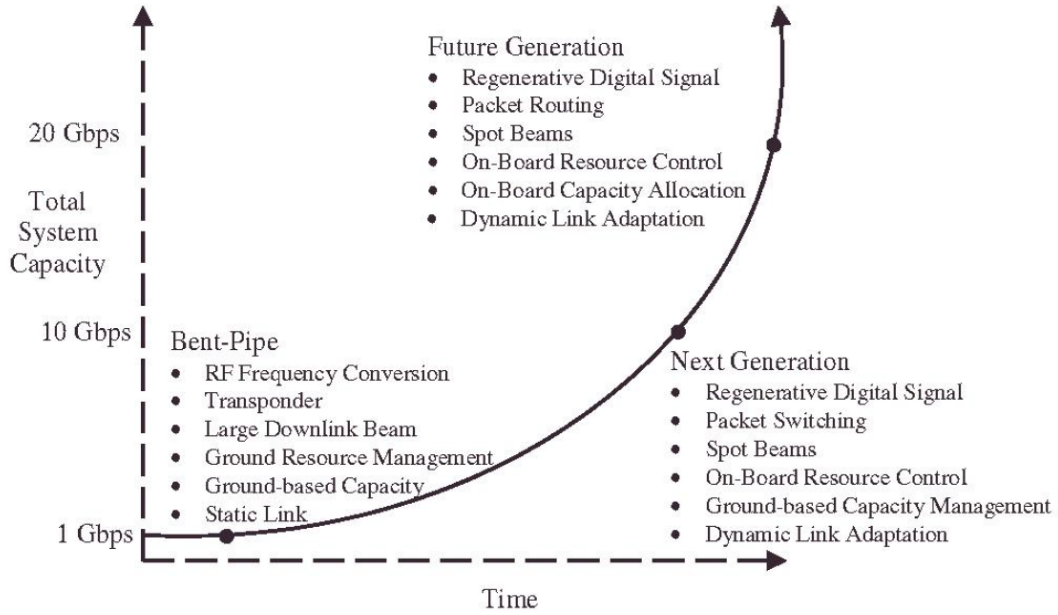
Figure 1-1: Generations of satellite systems [5]

munication satellites are spot beams. In a spot beam the signal power if focused on a specific area of the Earth's surface, being the beam's footprint in the order of several hundreds of kilometers. Next-generation high-throughput satellites (HTS) such as ViaSat-2 and EchoStar 24 provide 300 - 500 Gbit/s of capacity and have an increasing number of beams, since narrow ones provide more gain. Furthermore, phased-array antennas are being introduced to satellites, which allows changing the number of beams, their shape and size (beamforming).

However, the greater flexibility of new satellites has also incremented their complexity. With an increased number of beams, and multiple configurable variables for each of them (power, bandwidth, boresight pointing, etc.), advanced techniques for dynamic resource managment (DRM) are required. Since several companies such as SpaceX, Telesat, Intelsat or SES are planning to launch satellites with these characteristics, DRM has become a popular topic of research both in industry and academia.

16

1.2 Literature review

Recent literature has examined the issue of resource allocation in communications satellites and optimization [6]. A number of studies focus on beam hopping techniques [7], [8], [9] in which only a portion of the satellite beams are active at a given time. In particular, the authors in [7] propose a genetic algorithm to optimize the active beams' time plan whereas [8] and [9] analyze the advantages of applying beam hoping to conventional satellite systems.

Another area of research is cognitive satellite communications, which consists in monitoring the spectrum dedicated to other systems and exploiting this spectrum if it is not being used. Authors in [10], [11] and [12] propose beamforming [13] and bandwidth allocation in a spectral coexistence scenario of satellites and ground users.

Aravanis et al. [14] develop a hybrid genetic algorithm and simulated annealing method to minimize the unmet system capacity (USC) as well as the total power used, but bandwidth is allocated uniformly. In [15], besides power, carrier allocation is also considered to minimize the co-channel interference using an analytical approach based on the axiomatic interference model to balance the signal-to-interference-plus-noise ratio (SINR) [16]. The authors in [17] use the method of Lagrange multipliers to allocate power and bandwidth considering the delay bounds of real-time packages, although the system of study is just one link with few users. This type of delay-sensitive traffic is also considered in [18], where the authors present an algorithm based on the non-dominated sorting genetic algorithm II (NSGA-II). They obtain a Pareto front of the throughput and call completion ratio by allocating carriers, time slots and powers to packages. Nevertheless, they do not model interference between beams and just limit frequency reuse. In [19] the return link is optimized after satisfying the forward link requirements using, again, Lagrange multipliers. Based on the duality theory, the authors in [20] develop an iterative power and bandwidth allocation algorithm that penalizes delays but ignores interferences between beams.

After analyzing the literature, it can be concluded that there is a research gap in the area of multibeam-satellites algorithms that allocate both power and bandwidth

while considering important factors such as the interference between beams, which this thesis aims to cover.

1.3 Thesis objectives

The specific objectives of this thesis are:

- Analyze power and bandwidth influence on the performance of a communications satellite with and without interference and atmospheric attenuation.

- Develop a new methodology of power and bandwidth allocation in multibeam satellite systems extending the approach that [14] implemented for allocating only power.

- Investigate the performance improvement of dynamically allocating bandwidth as compared with previous studies where only power was allocated.

1.4 Thesis overview

This thesis consists of five chapters. Chapter 2 presents the system model and shows results on simple case studies. Chapter 3 states the problem this thesis aims to solve and outlines the proposed solution. The results obtained by performing simulations on the problem are shown in Chapter 4. Finally, Chapter 5 summarizes the main findings of this thesis and highlights opportunities for future research.

Chapter 2

System model

2.1 Communications satellites theory

This section explains the main theoretical concepts behind communications satellites so the reader can understand the rest of this thesis.

2.1.1 Link budget

Space communications are established through wireless links. To design them, engineers use an equation commonly termed the "link budget equation" that accounts for the gains and losses in power from the transmitter, through the different components of the medium and to the receiver. In other words, the link budget equation determines the received power after subtracting all the power losses to the transmit power. The link budget is shown in Equation 2.1:

$$P_r = \frac{P_t \cdot G_t \cdot G_r}{L_{fs} \cdot L_m} \tag{2.1}$$

Equation 2.2 shows the link budget with all the parameters in decibels, obtained after applying the logarithm in base 10 and multiplying by 10 the previous equation:

$$P_r = P_t + G_t - L_{fs} - L_m + G_r \tag{2.2}$$

where P_r is the power received, P_t is the transmitter power, G_t is the transmitter gain, L_{fs} and L_m are the free space and miscellaneous losses respectively, and G_r is the receiver gain. Miscellaneous losses are due to factors such as atmospheric attenuation (Subsection 2.2.3 outlines its contributions), implementation losses in the hardware components or polarization losses. Both gains are calculated as:

$$G = \eta \left(\frac{\pi D}{\lambda}\right)^2 \tag{2.3}$$

where η is the antenna efficiency, D is the antenna diameter, and λ is the signal's wavelength. L_{fs} is calculated as:

$$L_{fs} = \left(\frac{4\pi d}{\lambda}\right)^2 \tag{2.4}$$

where d is the distance from the transmitter to the receiver.

The transmit performance of an antenna is calculated by its effective isotropic radiated power (EIRP), which is the sum of the transmitter power and gain.

The achievable data-rate depends on the ratio between the received power and the noise power. The noise power at the receiver can be calculated as:

$$N = k T_{sys} B \tag{2.5}$$

where k is the Boltzmann constant, T_{sys} is the system noise temperature and B is the bandwidth the link uses. The system noise temperature is computed taking into account the antenna noise temperature, the atmospheric noise temperature, as well as the noise temperature of the LNB and the rest of components in the radio frequency (RF) chain. The signal to noise ratio or SNR is an important figure of merit calculated as P_r/N.

It is common in communication systems to express the SNR in terms of the energy per bit (E_b) and the noise spectral density (N_0). In particular the relationship between

the SNR and the $\frac{E_b}{N_0}$ is given by:

$$\frac{E_b}{N_0} = SNR + B - R_b \qquad (2.6)$$

where N_0 is N/B and R_b is the data rate measured in bits per second (Gbps in high-throughput satellites, HTS).

Finally, in any valid link budget, the $\frac{E_b}{N_0}$ needs to be greater than a $\frac{E_b}{N_0}$-threshold value (that depends on the modulation scheme used and the bit error rate desired) plus a certain margin γ, which is commonly set to 2 dB:

$$\frac{E_b}{N_0} \geq \left(\frac{E_b}{N_0}\right)_{threshold} + \gamma \qquad (2.7)$$

2.1.2   Data rate and spectrum

The electromagnetic spectrum is divided in bands, each one of them having a lower and an upper frequency (e.g., the Ka band goes from 26.5 GHz to 40 GHz). This spectrum is regulated by agencies such as United Nation's International Telecommunication Union (ITU). Communications satellites companies need to obtain licenses from the regulatory bodies to use a certain portion of spectrum which is commonly referred as the "available bandwidth" (the difference between the upper and lower frequencies).

The data rate that a certain beam provides is calculated with the following equation:

$$R_b = \Gamma(P) \cdot B \qquad (2.8)$$

where R_b is the data rate, Γ is the spectral efficiency of the MODCOD[1] the beam uses (measured in $bit/s \cdot Hz^{-1}$), P is the beam power and B is the bandwidth the beam uses. As shown, the spectral efficiency is a function of the power: higher powers yield higher ratios of energy per bit to noise power spectral density $\left(\frac{E_b}{N_0}\right)$ and thus

---

[1]The modulation and coding scheme or MODCOD is the technique employed to encode information. Examples of MODCODs used in the Digital Video Broadcasting - Satellite - Second Generation (DVB-S2) standard are QPSK-3/4, 8PSK-9/10 and 32APSK-11/15.

more complex MODCODs with higher spectral efficiencies can be used for the same bit error rate (BER).

Therefore, bandwidth and power are the most important resources available to communications satellites. Power, delivered through solar arrays, is divided for each beam. Bandwidth, on the other hand, can be reused with two strategies:

- Polarization-division multiplexing (PDM). Electromagnetic waves consist of an electric field component and an orthogonal magnetic field component. The direction of the electric field defines, by convention, the polarization of the wave. In general, this direction rotates. Antennas can be designed to receive or transmit a wave of given polarization with respect to the direction of propagation (right-hand/clockwise or left-hand/counter-clockwise) while isolating the orthogonal polarization. Therefore, two links can be established concurrently at the same frequency and endpoints [2].

- Frequency reuse by spatial separation. Beams that use the same frequency and project on areas that are close to each other have more interference the closer they are. Nevertheless, if their projections are far apart, the interference is low and the spectrum can be reused by separating beams that use the same central frequency.

A combination of polarization and central frequency is commonly called a color. Communications satellites have multiple colors, usually four: two polarizations and two central frequencies.

2.2   Model description

This section explains the Python model used in this thesis, as well as the assumptions made.

2.2.1   Block diagram

Figure 2-1 shows a diagram of the model and the main parameters that influence each block. First, the modulator module assigns a specific MODCOD, central frequency and bandwidth to the digital signal, as well as the roll off factor (the parameter of a filtering needed to transmit a digital signal). Then, the power amplifier amplifies the signal to the desired power value, taking into account the efficiency and the output backoff (OBO: the difference between the maximum output level in an amplifier and the actual value, needed to avoid saturation) of the power amplifier. The transmission antenna module computes the gain using the diameter, the efficiency and the frequency.

Afterwards, the signal leaves the satellite and crosses the channel. The path losses (L_{fs} in Equation 2.2), atmospheric attenuation and interferences (detailed in the following sections) are calculated. The model then computes the gain at the receiver antenna in the same manner as calculated for the transmitter. Finally, the low noise block (LNB) noise figure is taken into account to calculate the temperature of the system and the voltage standing wave ratio is used to reckon the LNB losses. As indicated in Figure 2-1, there are also radio frequency (RF) losses that correspond to the losses in the different physical components of the RF chain.

These link budget calculations are executed multiple times. First, an iteration is made with a low-spectral-efficiency MODCOD. If the link closes with a margin for the signal of at least 3 dB, the model is run again with the MODCOD that has the next higher value of spectral efficiency until this margin is not achieved. Therefore, the modulation that is finally chosen is the one that provides the highest data rate and still yields a 3 dB margin. This modulation is chosen from a total of 62 MODCODs defined in the Digital Video Broadcasting - Satellite - Second Generation Extensions (DVB-S2X) standard [21].
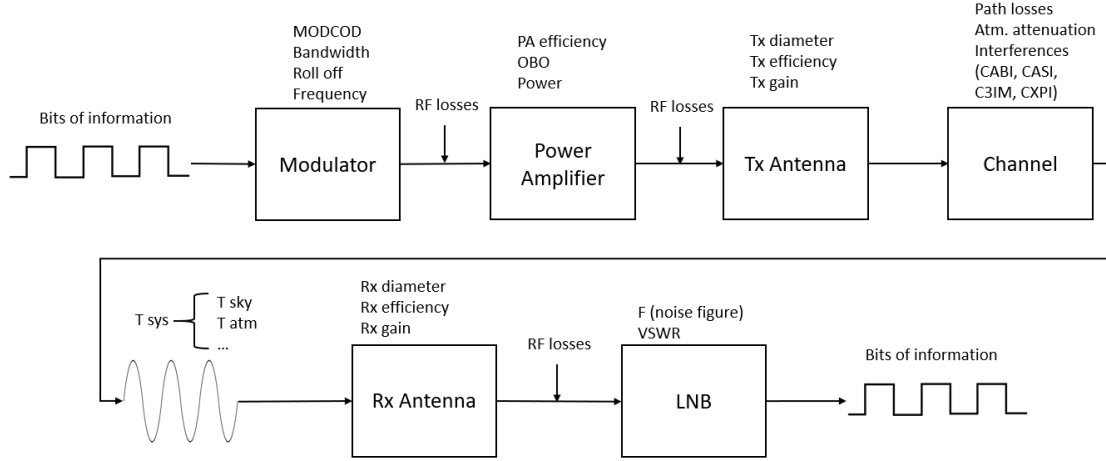
Figure 2-1: Model block diagram

2.2.2 Interferences

Interference is the effect of undesired signals or noise on the reception of a desired signal. The model implements several types of interference:

- **Adjacent beams interference.** Originates when multiple beams that are close to each other have the same polarization and central frequency, that is, the same color. The parameter that characterizes this interference is called Carrier to Adjacent Beam Interference ratio (CABI). An iterative process is followed to take into account this interference that consists in:

  1. Compute which beams that have the same color are adjacent to the current beam. Add this beams to the list "closest".

  2. While there is no change in all MODCODs or they change to previous visited values, for each beam:

     (a) Calculate, at the current beam's footprint center, how much power from the "closest" beams is received. For this calculation, the antenna radiation pattern recommended in [22] (second method) is implemented.

     (b) Calculate the CABI.

     (c) Compute the link budget.

24

- **Adjacent satellites interference.** Caused by other satellites with beam footprints that are near the system's footprints. This type of interference is not calculated, but assumed. The Carrier to Adjacent Satellites Interference ratio (CASI) defines it.

- **Cross polarization interference.** Although frequency can be reused by having two links with orthogonal polarizations, it is common that a fraction of the undesired orthogonal signal interferes with the received signal. As the CASI, this type of interference is not calculated. The parameter that characterizes it is the Carrier to Cross Polarization Interference ratio (CXPI).

- **Interference due to third order modulation products.** Because of nonlinearities in real-life systems, there are undesired amplitude modulations of signals containing two or more different frequencies, a phenomenon called intermodulation. The third-order intermodulation products are the ones that interfere the most, because of their amplitude and proximity to the signal frequency. The Carrier to Interference ratio due to Third order Modulation products (C3IM) defines this type of interference. The C3IM is calculated from the 32 APSk 3/4 1C C3IM vs IBO curve, found at [21]. The IBO − OBO ratio is assumed to be 1:1.

2.2.3   Atmospheric attenuation

Atmospheric attenuation is calculated according to ITU recommendations using data and statistics from where each beam is pointing. The different contributions to the atmospheric attenuation are:

- **Rain attenuation.** The most important fading mechanism at communications satellites bands [23], the worse the more it rains in the region. ITU-R recommendation P.618 [24] is implemented to compute this type of attenuation.

- **Ionospheric scintillation attenuation.** The ionosphere is part of Earth's upper atmosphere. This region is permanently ionized due to solar radiation,

and this phenomenon causes rapid modification of radio waves along with attenuation of the signal. The ITU-R recommendation that provides the methods to calculate scintillation attenuation is the P.618 [24].

- **Gaseous attenuation.** Caused in the troposphere due to interactions with its gas molecules. This attenuation is higher in the resonance frequencies of the molecules (i.e., 60 GHz band for oxygen molecules). ITU-R recommendation P.676 [25] outlines the calculations needed to compute the gaseous attenuation.

- **Cloud attenuation.** Water or ice particles present in clouds absorb and scatter the signal. Statistics about cloud presence, density, and particle size are used to calculate this type of atmospheric losses. ITU-R recommendation P.840 [26] is implemented to compute this type of attenuation.

To compute the atmospheric attenuation, the availability percentage is needed. This parameter is the fraction of time in which the atmospheric attenuation is lower than the calculated. For example, an availability of 95% signifies that the atmospheric attenuation value calculated by the model is only surpassed in real life 5% of the time.

2.3 Simple case studies

As explained previously, power and bandwidth per beam are the resources available on communications satellites that have a greater influence on their performance. The purpose of this section is analyzing how the allocation of both affects the data rate provided.

2.3.1 System specification

The parameters that are used for the simple case studies are defined in Table 2.1.

Different scenarios are considered. For the cases without interference, the CABI and C3IM equal 1000 dB. When interference is added to the system, they are com-

Table 2.1: System parameters for the simple case studies

Parameter	Value	Unit
Satellite orbit	Circular equatorial	-
Altitude	8063	km
Payload power (P_{tot})	50	W
Total bandwidth	2	GHz
Central frequency	25	GHz
Beam shapes	Circular	-
Number of beams	2	-
Roll off	0.1	-
PA efficiency	0.65	-
Tx antenna diameter	1	m
Tx efficiency	0.65	-
Tx losses	0.75	dB
Rx antenna diameter	1	m
Rx efficiency	0.65	-
Rx losses	0.75	dB
Rx antenna temperature	290	K
LNB noise figure (F)	3	-
LNB Voltage Standing Wave Ratio	1.2	-
Availability	99	%
CASI	1000	dB
CXPI	1000	dB

puted. The performance metric M is calculated as:

$$M = \sum_{b=1}^{N} R_b \quad \text{s.t.} \quad R_b \leq D_b \tag{2.9}$$

where R_b and D_b are the data rate provided by the satellite and the demand requested by users respectively, in Gbps. N is the number of beams.

Different conditions of demand are studied: low demand and high demand. Low demand means consumers only use around 20% of the total system capacity. On the other hand, high demand means consumers' requests surpass the system capacity.

Figure 2-2 shows the system of study. Both beams have the same color and thus interfere. The distance between their center is equal to one circle's diameter, 115 km, since this is approximately how beams with the same color are spaced in a system with more beams.

The following subsections present 16 scenarios:

- **4 demand cases:** all the combinations of demand of beam 1 (D1) high/low and demand of beam 2 (D2) high/low.

- **2 interference scenarios:** without/with interference.

- **2 atmospheric attenuation scenarios:** without/with atmospheric attenuation.

In the next subsection, each figure is generated executing the model with 20 different values of power and bandwidth for beam 1 (beam 2 receives the total resources minus the resources allocated for beam 1). For each figure, the vertical axis shows the power allocated to beam 1, whereas the horizontal axis shows the bandwidth allocated to the same beam. The points that yield the highest data rate for the satellite (sum of the data rate of beam 1 and beam 2) are indicated with a black dot and the data rate is shown in Gbps, except if there are more than 6 optimal points.
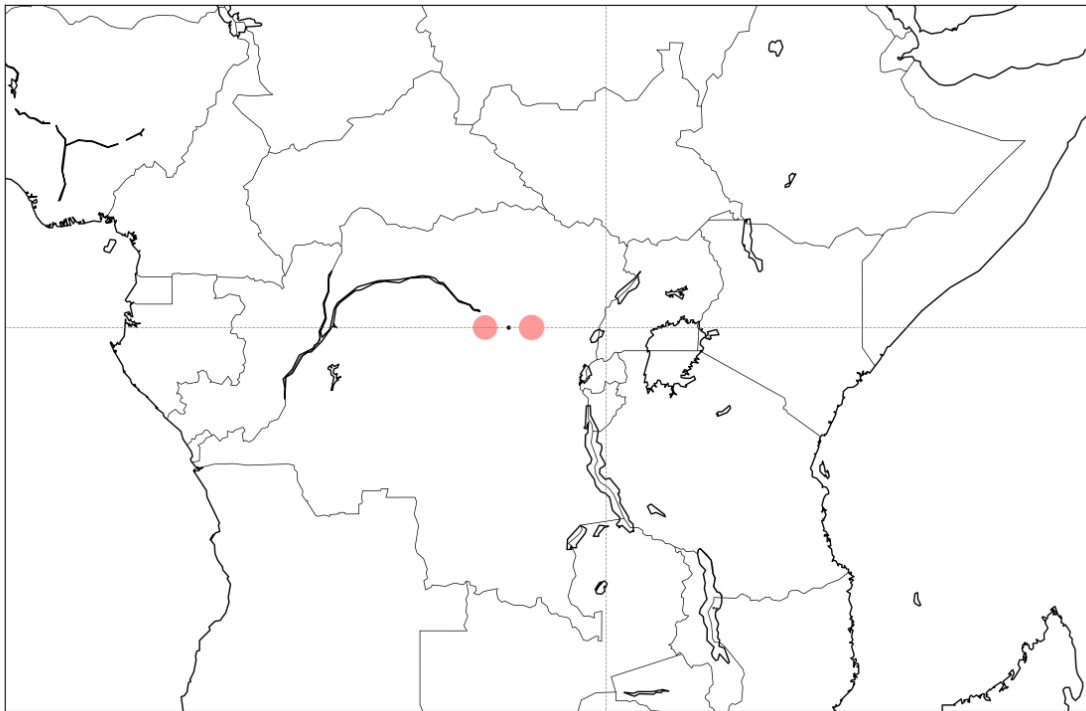
Figure 2-2: System of study: a satellite over Africa with 2 beams (115 km in diameter) colored in red. The satellite projection falls just between them, indicated with a small dot.

2.3.2 Cases without atmospheric attenuation

Without atmospheric attenuation, beam communication links are identical and therefore symmetry can be observed.

D1 high, D2 high

Without interference   Figure 2-3 shows the performance is highest in 2 points close to the diagonal (that is, the optimum is to give a proportional amount of power and bandwidth to a beam). Instead of allocating resources equally, a higher performance is achieved when giving around 70% of the total power and bandwidth to a single beam. The reason for this behavior is explained in Subsection 2.3.4.

With interference   Figure 2-4 presents the results obtained for this case, which are similar to the case without interference. Nonetheless, due to interference, a strategy that yields a greater performance is now to assign a higher percentage of resources to a single beam. This behavior is expected: the other beam is weaker and does not interfere as much.

D1 high, D2 low

Without interference   In Figure 2-5 it can be observed that, as intuition would indicate, the vast majority of resources are given to beam 1 to satisfy its high demand.

With interference   If interference is added to the previous case, performance decreases slightly although the optimal combination of power and bandwidth is very similar to the case without interference. The result is shown on Figure 2-6.

D1 low, D2 high

Without interference   As expected, this case is symmetric with the D1 low D2 high scenario without interference shown in Figure 2-5, since beam links are identical.
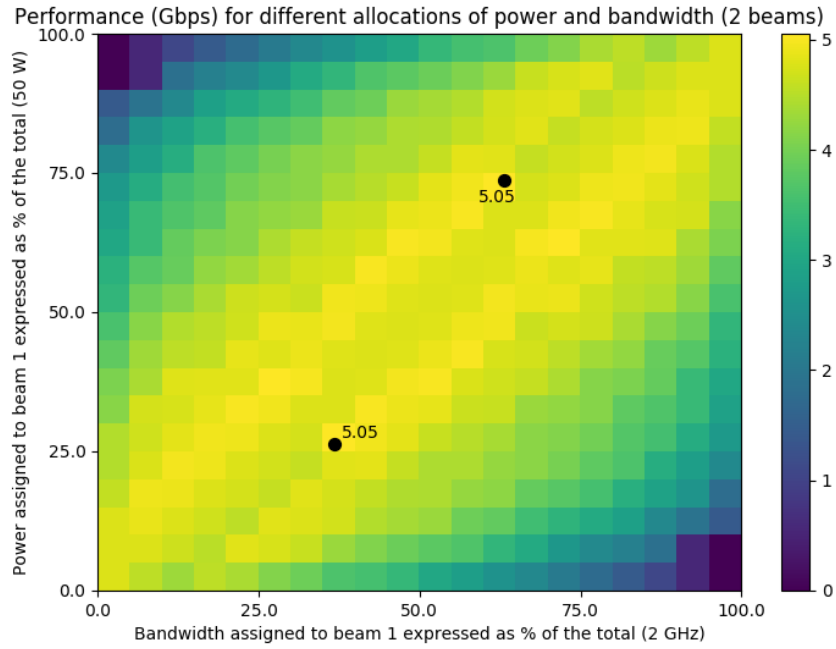
Figure 2-3: D1 high, D2 high, no interference, no atmospheric attenuation
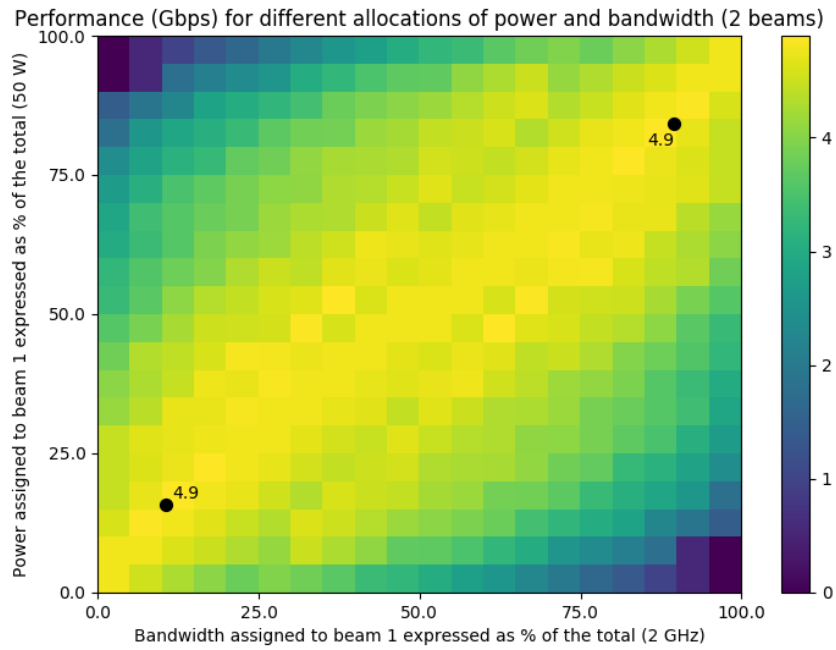

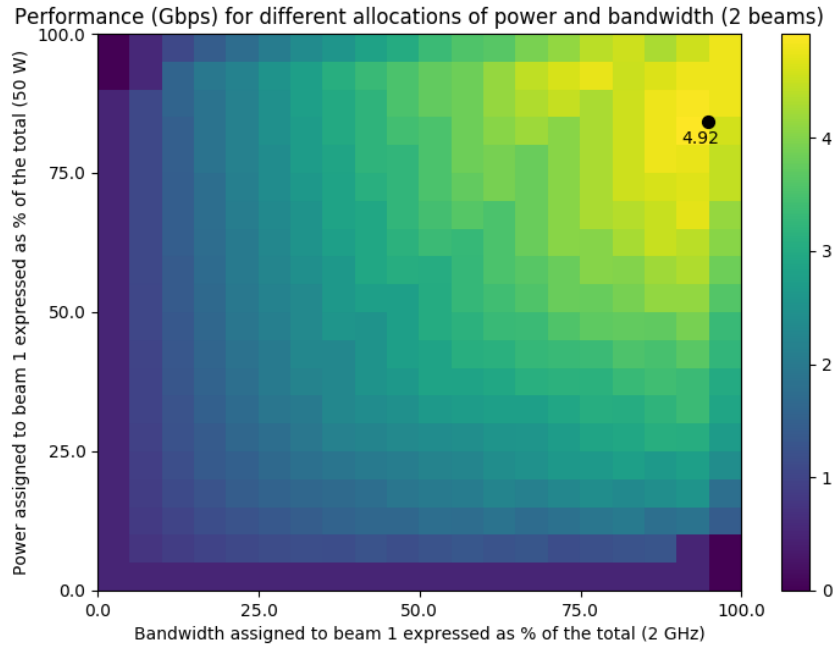Figure 2-4: D1 high, D2 high, interference, no atmospheric attenuation

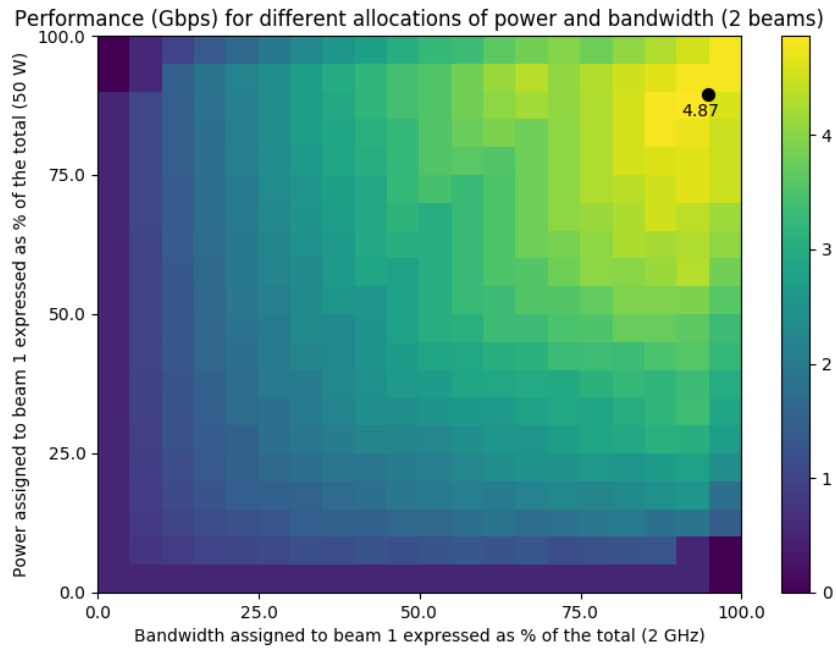Figure 2-5: D1 high, D2 low, no interference, no atmospheric attenuation

Figure 2-6: D1 high, D2 low, interference, no atmospheric attenuation

Thus, the results are not shown. Instead of giving most of the resources to beam 1, the system prefers giving a high power and bandwidth to beam 2.

With interference   Again, this case is symmetric with the D1 high D2 low scenario with interference shown in Figure 2-6. The performance decreases slightly when adding interference but the optimal point remains close to the previous case. Results are not displayed.

D1 low, D2 low

Without interference   Figure 2-7 shows the maximum performance is just 1.01 Gbps, obtained at many points (not marked to avoid cluttering). Since the system is capable of satisfying the demand by far, almost every combination of power and bandwidth assigned is optimum.

With interference   Again, the best performance is 1.01 Gbps. Figure 2-8 shows the results for this case, which is very similar to the previous one but now slightly less combinations of power and bandwidth provide the optimum performance due to interference.

2.3.3   Cases with atmospheric attenuation

The addition of atmospheric attenuation causes beam communication links to be different, since they are not pointing at the same latitude and longitude on the surface of the Earth. Thus, one beam can have a higher attenuation than the other one due to factors such as more frequent rain or clouds in the area, to name two examples.

D1 high, D2 high

Without interference   In this system, beam 1 has more attenuation than beam 2. Figure 2-9 shows that, therefore, the best performance is obtained when all the resources are given to beam 2.
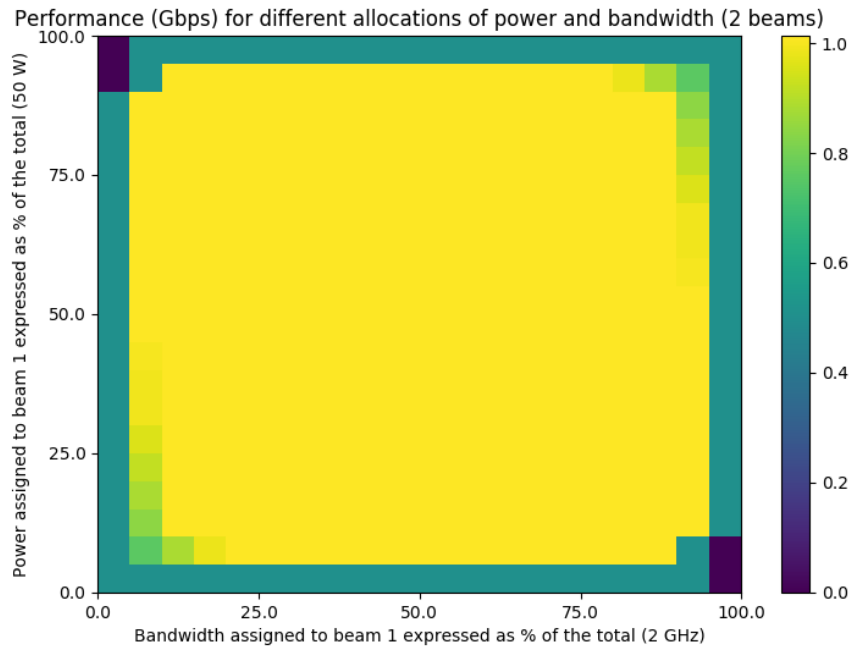
Figure 2-7: D1 low, D2 low, no interference, no atmospheric attenuation

Figure 2-8: D1 low, D2 low, interference, no atmospheric attenuation
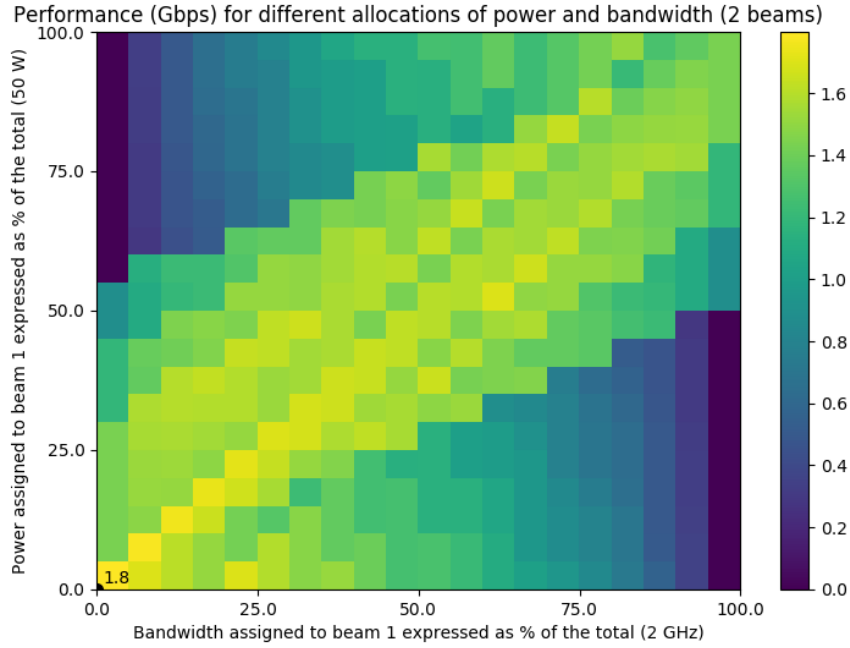
Figure 2-9: D1 high, D2 high, no interference, atmospheric attenuation

With interference   Since atmospheric attenuation is much higher than interference, this case has minor differences with the previous one. The result can be observed in Figure 2-10.

D1 high, D2 low

Without interference   Figure 2-11 shows this case. As stated before, beam 2 has less attenuation. Therefore, even though its demand is low, the system performance is more optimal when a fair amount of resources to beam 2 is given to satisfy its demand, and the rest to beam 1. This is in contrast to the D1 high, D2 low case without atmospheric attenuation, where the beam with the highest demand was the one to receive the vast majority of power and bandwidth in the optimal point.

With interference   Again, interference is a small factor compared to atmospheric attenuation and therefore the results are almost the same than in the previous case, with minor differences. Figure 2-12 depicts them.
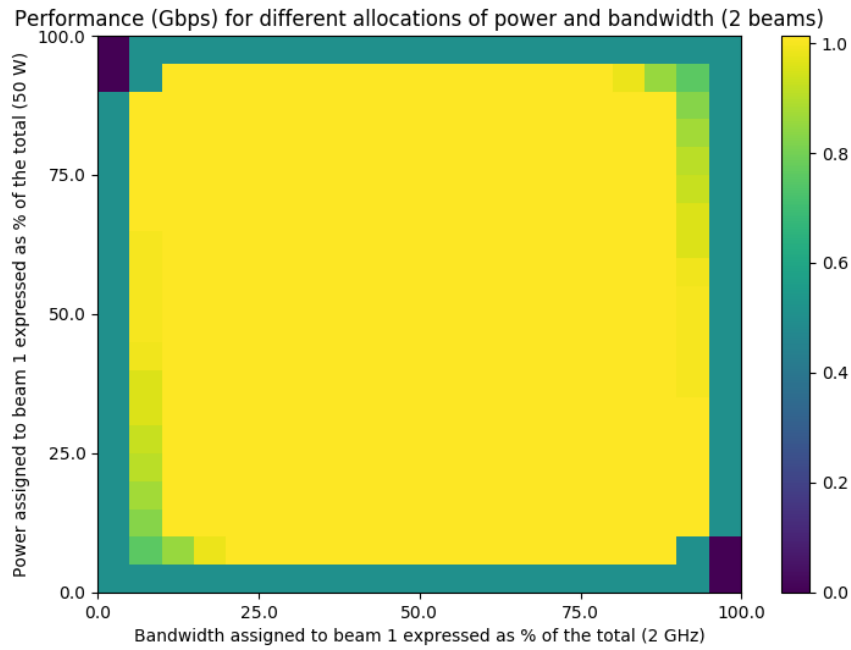
Figure 2-10: D1 high, D2 high, interference, atmospheric attenuation

Figure 2-11: D1 high, D2 low, no interference, atmospheric attenuation
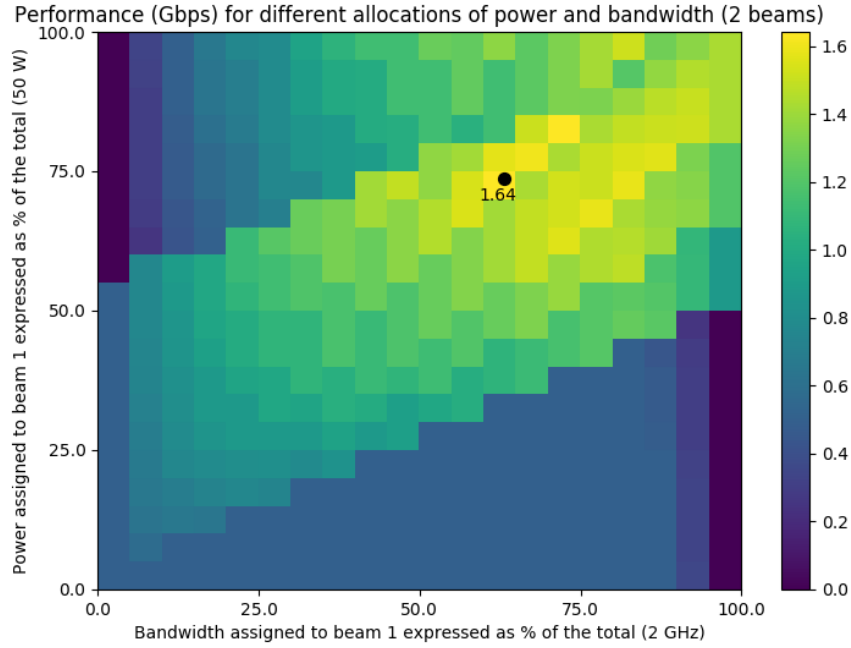
Figure 2-12: D1 high, D2 low, interference, atmospheric attenuation

## D1 low, D2 high

Without interference   Figure 2-13 presents the results obtained. As opposed to the case without atmospheric attenuation, now symmetry with the D1 high, D2 low is not observed. All the resources are given to beam 2 as expected: beam 2 has the highest demand and the least attenuation.

With interference   The results are similar than the previous case when interference is added to the system. Figure 2-14 shows these results.

D1 low, D2 low

Without interference   Figure 2-15 shows the maximum performance is 1.01 Gbps at many points, not marked to avoid cluttering. The number of points that provide this performance is lower, as expected, than in the case with no atmospheric attenuation (Figure 2-7) since this system is more constrained.
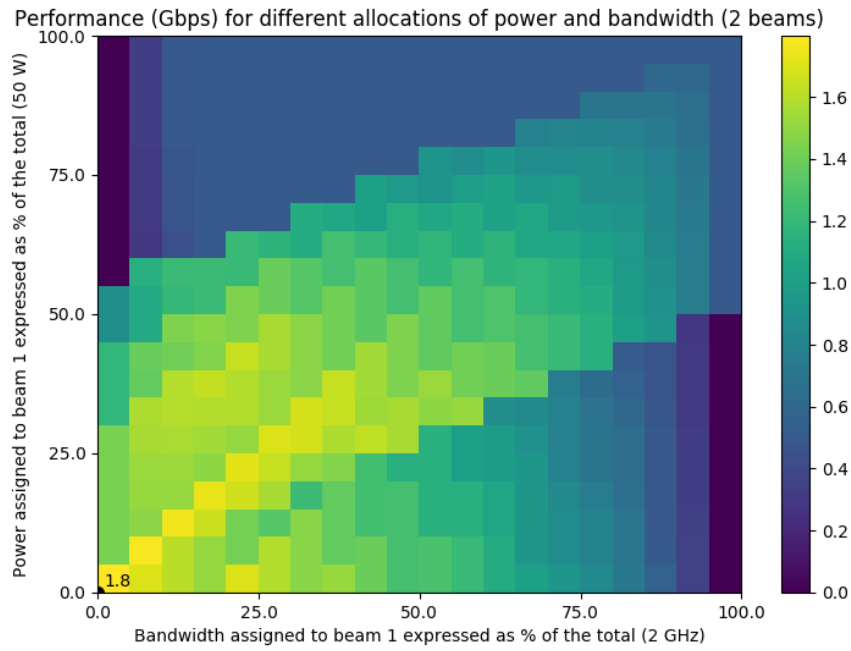
Figure 2-13: D1 low, D2 high, no interference, atmospheric attenuation
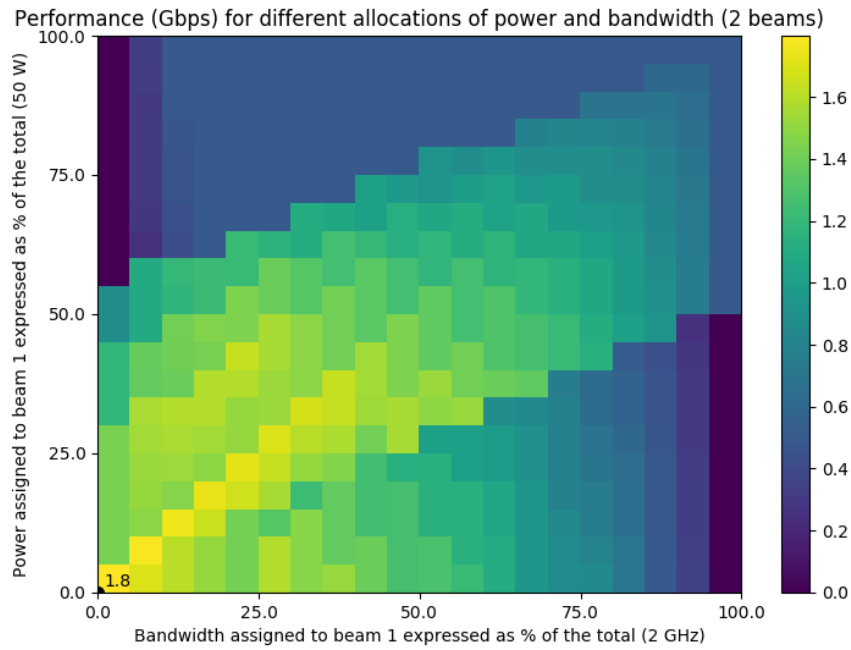
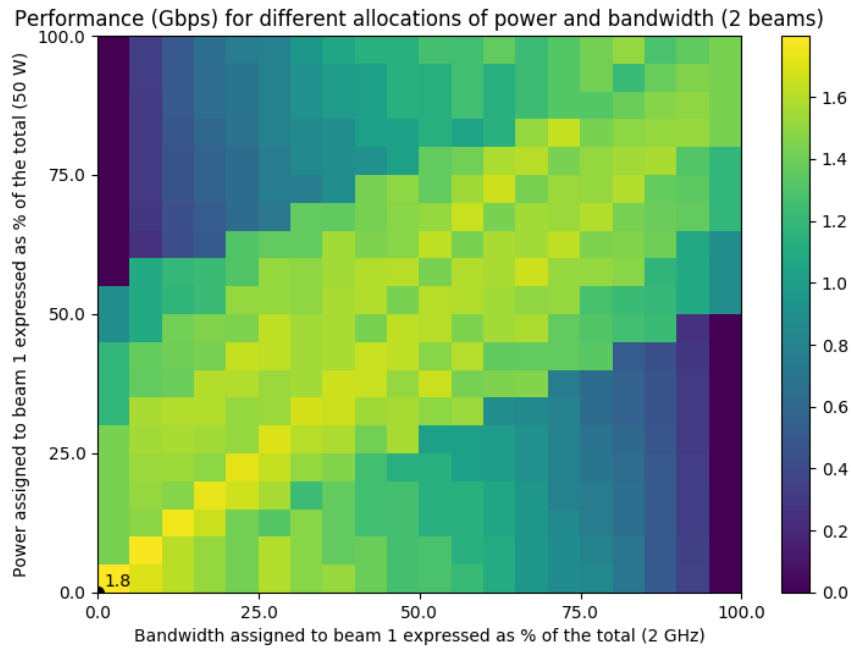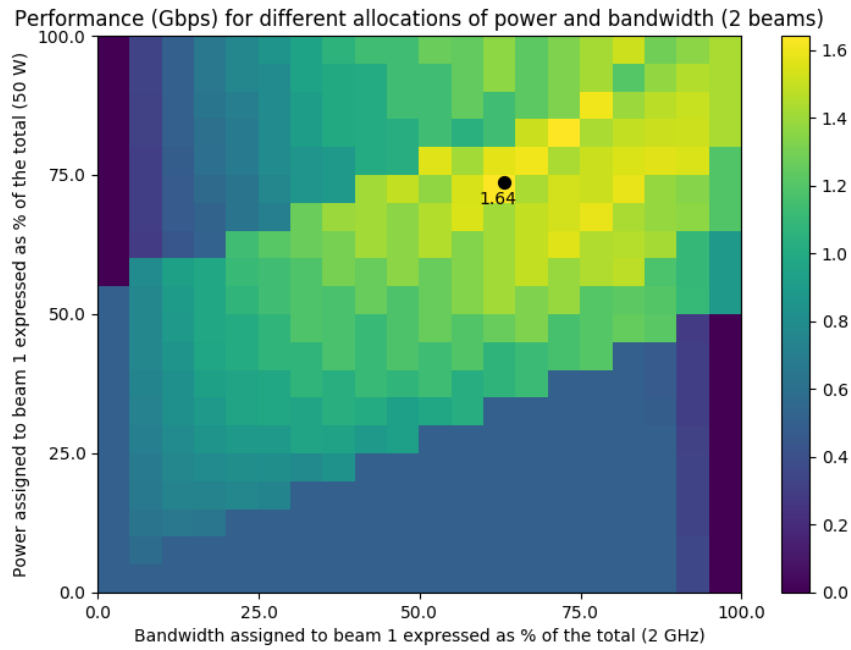Figure 2-14: D1 low, D2 high, interference, atmospheric attenuation
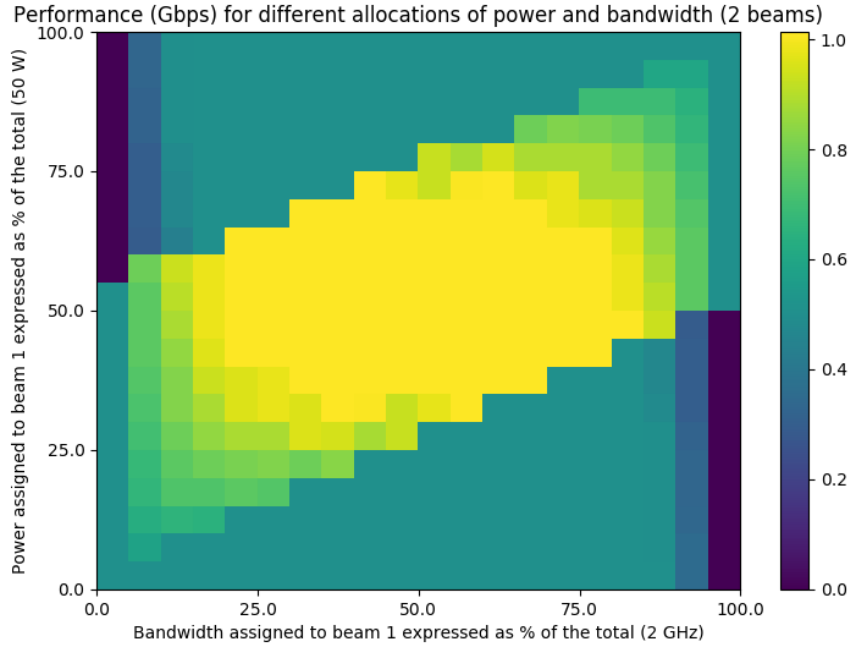
Figure 2-15: D1 low, D2 low, no interference, atmospheric attenuation

**With interference**   Figure 2-16 depicts this case. The maximum performance is, again, 1.01 Gbps obtained at many points. The effect of adding interference is that, like in the case without atmospheric attenuation, less combinations of power and bandwidth provide the optimum performance.

Table 2.2 summarizes the results shown previously. High and low demands are expressed with letter "h" and "l" respectively. "Atm. att." stands for atmospheric attenuation and "int." stands for "interference".

2.3.4   Power and data rate study

The previous cases show that a proportional amount of power and bandwidth should be given, and thus the optimal performance points are around the diagonal. This is the expected behavior, since both power and bandwidth (which are coupled) are influential parameters to establish a communications link.

Nevertheless, the optimum performance points are not exactly in the diagonal, which might seem the most intuitive behavior. For example, in Figure 2-3 the op-

Table 2.2: Summary of the results obtained in the simple cases

Case	Figure	Short description
No atm. att.		
D1 h D2 h no int.	2-3	The optimum is close to the diagonal, allocating around 70% of resources to a beam
D1 h D2 h int.	2-4	Similar to 2-3, but the best strategy is to assign a higher percentage of resources to one beam
D1 h D2 l no int.	2-5	Almost all resources are given to beam 1
D1 h D2 l int.	2-6	Slight decrease in performance but optimum point is similar to 2-5
D1 l D2 h no int.	-	Symmetrical to 2-5
D1 l D2 h int.	-	Symmetrical to 2-6
D1 l D2 l no int.	2-7	Many points provide the maximum performance
D1 l D2 l int.	2-8	Similar to 2-7 but slightly less points are optimum
Atm. att.		
D1 h D2 h no int.	2-9	The optimum strategy is to give all resources to beam 2 (which has less atmospheric attenuation)
D1 h D2 h int.	2-10	Minor differences with 2-9
D1 h D2 l no int.	2-11	Even though beam 2 has a low demand, the optimal point consists in giving a fair amount of resources to this beam
D1 h D2 l int.	2-12	Minor differences with 2-11
D1 l D2 h no int.	2-13	All the resources are given to beam 2
D1 l D2 h int.	2-14	Minor differences with 2-13
D1 l D2 l no int.	2-15	The maximum performance is obtained at many points, but less points than in 2-7
D1 l D2 l int.	2-16	Similar to 2-15 but slightly less points are optimum
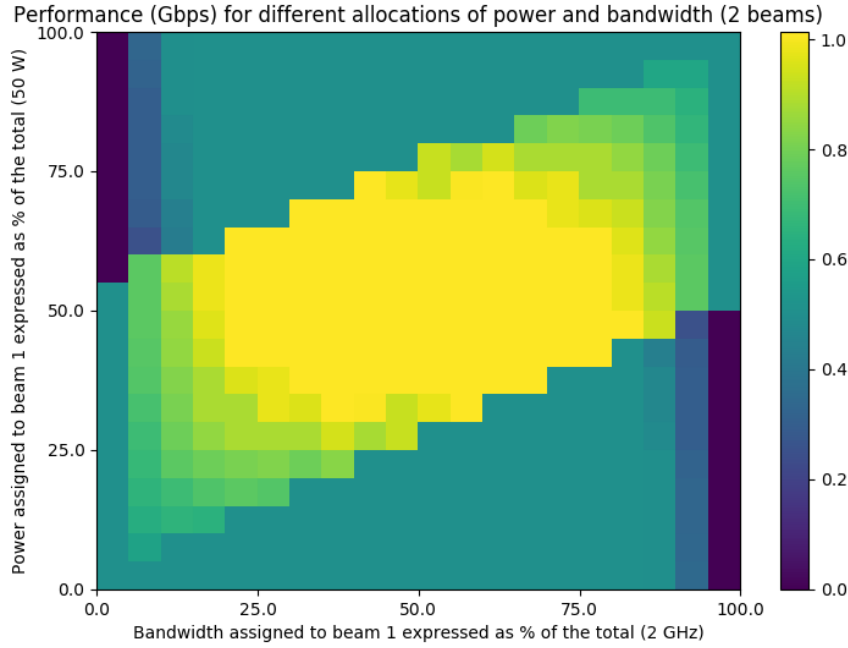
Figure 2-16: D1 low, D2 low, interference, atmospheric attenuation

timum points, colored in yellow, are just next to the diagonal. Since beams are identical, allocating power or bandwidth to one beam or another should not result in any difference. Therefore, the optimum should be in the diagonal.

As the demands of both beams are high, the performance metric calculated with Equation 2.9 is just the sum of each beam's data rate. As shown in Equation 2.8, the data rate is the product of the spectral efficiency and bandwidth. While bandwidth can be considered continuous[2], spectral efficiencies are not: this model considers 62 MODCODs and each of them has its specific value of spectral efficiency.

Figure 2-17 presents the relationship between data rate and power for a beam with fixed bandwidth. Two types of nonlinearities can be seen: discontinuities (each step represents a change in the MODCOD used) and a diminishing returns curve. As explained in Subsection 2.1.2, when power is increased the $\frac{E_b}{N_0}$ is increased as well. Thus, MODCODs with higher spectral efficiencies can be employed for the same BER. The optimal points are not in the diagonal because for a fixed bandwidth, the

---

[2]In real systems, bandwidth can only be assigned in portions of a few MHz. Since these cases dealt with Gbps of bandwidth, this issue does not affect the results.
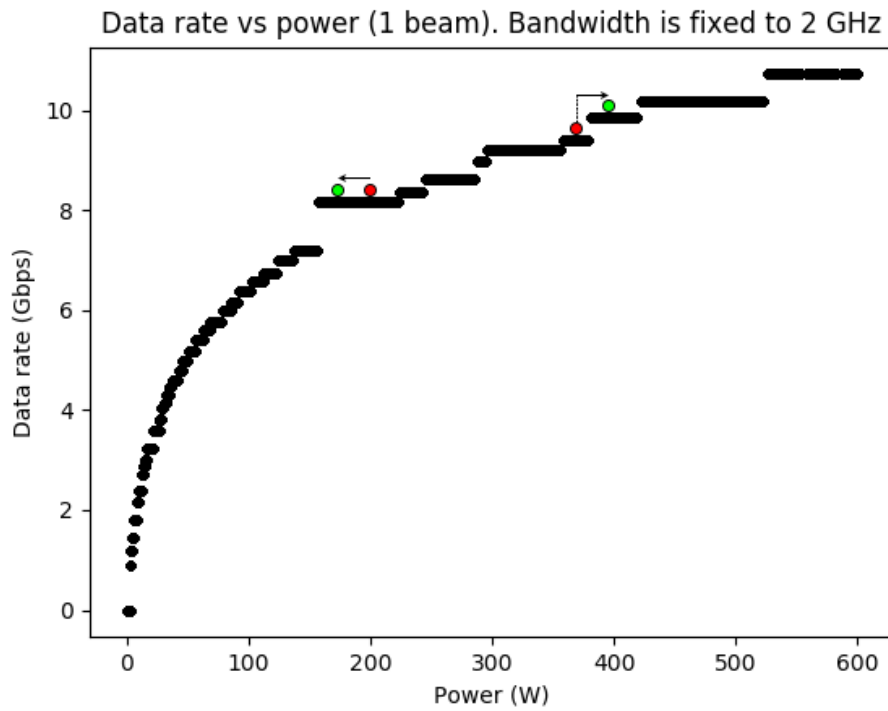
Figure 2-17: Data rate and power diagram for a beam that uses 2 GHz of bandwidth. For values of power higher than 600 W, the data rate is constant: the MODCOD with the highest spectral efficiency (256 APSK 3/4) is already achieved at 520 W.

optimum is to give additional power to a certain beam so this beam can use the adjacent MODCOD with higher spectral efficiency while reducing the power of the other beam which continues using the same MODCOD as before, like the green dots show. The red dots indicate suboptimal allocations for both beams, an allocation that could be in the diagonal.

Chapter 3

Problem statement

While the previous analysis was useful for understanding how power and bandwidth affect the performance of a communications satellite, real-world satellite systems present a much higher complexity. Satellites consist of several beams, each one having different values of power, bandwidth, polarization (left-hand or right-hand circular) and central frequency. This section presents the real-world problem that this thesis aims to solve.

3.1 Objective

Instead of using the metric calculated by Equation 2.9, the met system capacity (MSC), the unmet system capacity (USC) shown in Equation 3.1 is adopted for this problem. This metric, defined in [27], is used in this thesis' baseline reference, [14]. The USC is a more suitable metric because of its economic significance, since communications satellites companies have penalizations for not meeting their service-level agreements (SLAs) and thus their interest is to minimize the USC.

$$USC = \sum_{b=1}^{N} max[D_b - R_b, 0] \tag{3.1}$$

Figure 3-1 presents the relationship between the MSC and the USC. If the demand D_b is higher than the data rate R_b, the sum of the MSC and the USC equals the

demand. On the other hand, if the demand is lower than the data rate, the MSC equals the demand and the USC is 0.

The satellite has a specified central frequency and bandwidth available that can be reused as explained in Section 2.1, a total power P_{tot}, and a maximum transmit power per beam P_b^{max}. The objective of this problem is to minimize the USC (Equation 3.1) by allocating power and bandwidth to beams in a satellite subject to the constraints:

$$\sum_{b=1}^{N} P_b \leq P_{tot} \tag{3.2}$$

$$P_b \leq P_b^{max} \tag{3.3}$$

where P_b is the transmit power of beam b and N is the number of beams. Equation 3.2 ensures the beams do not use more power than what is available. Equation 3.3 is needed because power amplifiers have a saturation power value: above this value, distortion begins to occur.

3.2   Proposed solution: genetic algorithm

NP (non-deterministic polynomial time) is the class of decision problems for which solutions can be verified in polynomial time by performing deterministic computations [28]. P is the class of decision problems that can be solved in polynomial time. It is commonly though that P is not NP [29], and thus polynomial-time algorithms for NP problems are not believed to guarantee the reach of optimality. NP-hard problems are "at least as hard as the hardest problems in NP".

As demonstrated on [14], the NP-hard sum rate maximization problem is a special case of the resource allocation (RA) problem stated in this chapter. Furthermore, since the sum rate maximization problem can be reduced to the maximum independent set problem (which is hard to approximate[1]), it is demonstrated that this RA problem is also hard to approximate [14]. Therefore, using efficient and advanced metaheuristic optimization methods is appropriate.

---

[1]That is, approximation algorithms generate poor solutions.
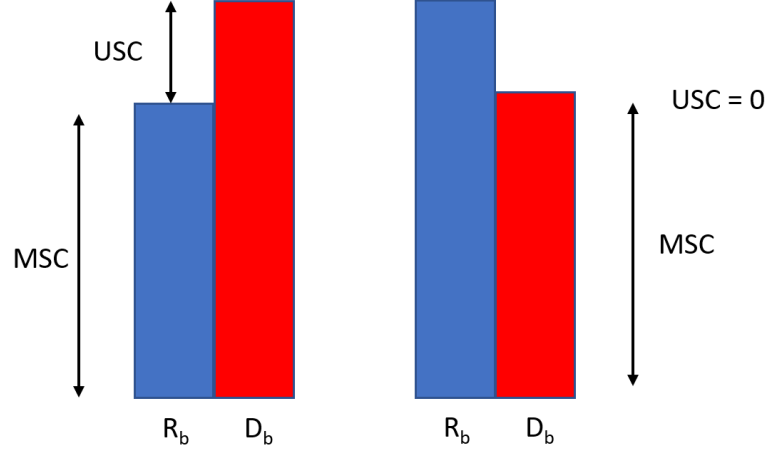
Figure 3-1: MSC and USC

Genetic algorithms are metaheuristic artificial intelligence techniques inspired by biological evolution [30]. A set of "individuals" (that is, solutions to the problem) are generated and evolved through random processes similar to the ones found in nature such as:

- Mutation. It causes attributes of the individual to be changed randomly, giving the algorithm the possibility to reach diverse solutions.

- Crossover. It uses two individuals (the parents) to stochastically generate a new individual.

- Selection of the fittest. On every generation of the genetic algorithm, after applying the mutation and crossover operators, the best individuals from the population (that is, the solutions that have a higher performance or fitness) are more likely to be chosen as the population for the next generation.

In this problem, each individual consists of a particular power and bandwidth allocation for each beam in the satellite, and its fitness (that has to be minimized) is the USC.

Since the genetic algorithm approach followed on [14] provided better results than the simulated annealing, particle swarm or differential evolution techniques, the proposed solution adopts this approach not only for allocating power to satellite beams

but also to allocate bandwidth. To implement the genetic algorithm in Python, the Distributed Evolutionary Algorithms in Python (DEAP) framework is used [31], which provides functions to fully customize evolutionary algorithms. It is compatible with parallelization tools such as the Python Standard Library multiprocessing package (which is used in this thesis) and the Scalable Concurrent Operations in Python (SCOOP) distributed task module [32] which allow parallel evaluations of the individuals fitness.

Algorithm 1 presents an overview of the method implemented. Initially, the genetic algorithm creates new individuals by assigning random values of power and bandwidth – within a certain range – to the beams (every attribute of an individual is a power and bandwidth allocation for a beam) and evaluates these individuals. Then, the following process is executed iteratively: for each generation, the population is selected, crossover and mutation are applied and the individuals changed are evaluated (fitness is invalidated if the individual was applied crossover or mutation). There are two termination conditions for the algorithm:

- Reaching *ngen* generations. A maximum number of generations sets an upper limit in the algorithm's execution time, needed to obtain solutions in a timely manner.

- Reaching *nmin* generations and having an improvement of less than *threshhold* between two consecutive solutions in the last three generations. This convergence criteria is needed so the algorithm is unbiased in determining when to stop in different demand scenarios. Moreover, there are cases in which the USC might increase slightly and decrease in the following generation, so a window of three generations is a better approach than just considering the difference between two generations. Furthermore, a minimum number of generations *nmin* should be set to help the algorithm reach better solutions.

The constraint handling techniques, needed to comply with Equations 3.2 and 3.3 as well as to avoid frequency overlap, depend on the number of beam colors and are thus described in the following section.

Algorithm 1 Genetic algorithm to allocate power and bandwidth

1: **function** EVALUATE_SOLUTION(ind)
2:     ind = constraint_handling(ind)
3:     sat = Satellite(ind)
4:     $sat.run\_link\_budget()$
5:     **return** USC(sat)

6:
7: $pop \leftarrow$ list of $nind$ individuals generated randomly
8: **for** ind in pop **do**
9:     $ind.fitness$ = evaluate_solution(ind)
10: $gen = 1$
11: **while** $gen \leq ngen$ **do**
12:     $offspring$ = selection_tournament(pop)
13:     $offspring$ = crossover_and_mutation($offspring$)
14:     **for** ind in pop **if** not $ind.fitness.valid$ **do**
15:         $ind.fitness$ = evaluate_solution(ind)
16:     $pop \leftarrow offspring$

17:
18:     **if** $gen \geq nmin$ **then**
19:         min_1 =min_USC(gen)
20:         min_2 =min_USC($gen - 1$)
21:         min_3 =min_USC($gen - 2$)
22:         $improv\_1$ =max($min\_2 - min\_1, 0$)/min_2
23:         $improv\_2$ =max($min\_3 - min\_2, 0$)/min_3
24:         **if** $improv\_1 < thresh$ and $improv\_2 < thresh$ **then**
25:             **break**
26:     $gen \leftarrow gen + 1$
27: **return** pop

Chapter 4

Results from the problem

In this section, results from the problem explained previously are presented.

4.1   System and algorithm specification

The system parameters are the same as the ones from the system described in Section 2.3 (presented in Table 2.1) except for the parameters shown in Table 4.1. The changes were made to better approximate the system in [14].

Figure 4-1 displays the communications satellite system. Beams have a specific color out of 4 possibilities: 2 polarizations and 2 central frequencies. Colors red and green have a left-hand circular polarization (LHCP), while colors yellow and blue feature a right-hand circular polarization (RHCP). Beams with different polarizations are independent, while beams that are both LHCP or RHCP can trade bandwidth between them if they are adjacent. Figure 4-2 shows an example: a red beam can increase its bandwidth if the green beams that are adjacent have their bandwidth reduced (to avoid interference due to links using frequency intervals that overlap).

Table 4.2 shows the parameters used in the genetic algorithm. The selection of the new population, done in the beginning of every generation, is by tournament with size 5. That is, the best individual out of a random group of 5 is chosen and this is repeated 1000 times, the population size. The crossover between two individuals occurs with a probability of 95%. This crossover is uniform with an independent

Table 4.1: System parameters for the problem

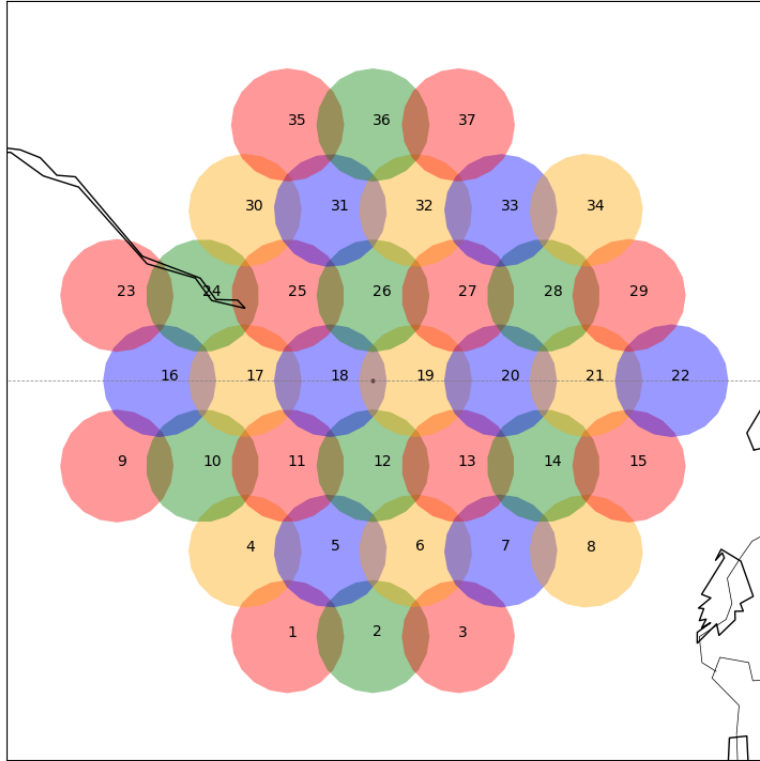| Parameter	Value	Unit
Payload power (P_{tot})	2350	W
Maximum power per beam (P_b^{max})	100	W
Total bandwidth	3	GHz
Central frequency	20	GHz
Number of beams	37	-
Tx antenna diameter	2.4	m
Rx antenna diameter	0.7	m
Rx antenna temperature	207	K
Availability (to calculate atmospheric attenuation)	50	%
CASI	30	dB
CXPI	30	dB

Figure 4-1: Plot of the satellite (black dot in the center) and its 37 beams (with a 4-color frequency reuse pattern). The system is on the equator over Africa, more specifically over the Democratic Republic of the Congo.
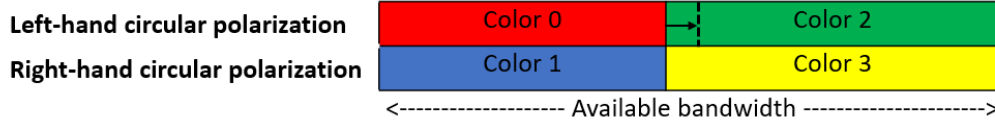
Figure 4-2: Colors and bandwidth diagram. Colors red and green have a LHCP, while colors blue and yellow have a RHCP. Adjacent beams that have the same polarization can trade bandwidth.

probability of 50%, that is, the resulting individual contains on average 50% of each parents' attributes (allocations of power and bandwidth for a beam). The mutation is uniform: when applying this operator, every attribute in an individual has a 15% probability of changing the values of power and bandwidth to new values uniformly chosen. Mutation is applied on 5% of individuals.

Table 4.2: Genetic algorithm parameters

Parameter	Value
$ngen$	40
$nmin$	15
Population size	1000
Selection	Tournament
Tournament size	5
Crossover	Uniform
Crossover prob.	0.95
Crossover ind. prob.	0.5
Mutation	Uniform
Mutation prob.	0.05
Mutation ind. prob.	0.15

As explained in Section 3.2, the genetic algorithm assigns random values of power and bandwidth (within a certain range) to the beams. Therefore, it can generate solutions that are not correct, and thus have to be treated carefully. Several techniques to handle constraints in genetic algorithms are suggested [33], including rejection, reparation and penalization of invalid individuals. The approach this thesis takes is to repair the incorrect solutions.

For the beam power, the constraints are shown on Equations 3.2 and 3.3. Equation 3.3 is always satisfied since the initial generation and mutation functions already limit the random power assignation from 0 to P_b^{max}. The crossover function does not

53

assign new values of power (it only combines features from two solutions) and thus it cannot violate this constraint.

If the sum of the beam powers exceeds P_{tot}, the beam powers are multiplied by P_{tot}/sum to ensure solutions satisfy Equation 3.2. By performing this multiplication, the powers are proportionally reduced so that their sum is exactly P_{tot}.

As for bandwidth, the constraint is that every pair of adjacent beams should not have overlapping frequencies. That is:

$$B_a + B_b \leq B_{tot} \quad \text{for each adjacent and equally-polarized pair of beams (a,b)} \quad (4.1)$$

where B_a and B_b are the bandwidths allocated to beams a and b, and B_{tot} is the total satellite bandwidth. To enforce this constraints, every pair of adjacent beams with the same polarization (a, b) is checked. First, it is chosen to start from beam number 1 or 37 with 50% probability. When starting from beam 1, b is $a + 1$ (pairs are checked in an increasing order of beam IDs, from 1 to 37). On the other hand, when starting from beam 37, b is $a - 1$. Then, if $B_a + B_b > B_{tot}$, the algorithm assigns to B_a the result of $B_{tot} - B_b$ (that is, B_a is reduced). This procedure ensures that, when all pairs are handled, there are no violations of Equation 4.1.

Still, this technique might leave bandwidth unused. Figure 4-3 depicts an example of this phenomenon in beams 1, 2 and 3 (see Figure 4-1). Beams 1 and 3 have the same central frequency, while beam 2 has a higher one. The unused bandwidth between a triplet of beams can be calculated with Equation 4.2:
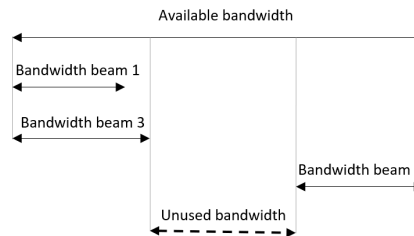

Figure 4-3: Example of a case in which the bandwidth is not completely used in beams 1, 2 and 3.

$$B_{unused} = B_{tot} - B_c - max(B_l, B_r) \tag{4.2}$$

where B_{unused} is the bandwidth not being used, B_{tot} is the total satellite bandwidth and B_l, B_c and B_r are the bandwidths of a triplet of adjacent beams (left, center, right).

To maximize the performance, the algorithm iterates over all the beams in a decreasing order of demand and increases their bandwidth by adding B_{unused}, which is always higher or equal than 0. After this procedure, it can be assured that there are neither interferences due to frequency overlap or bandwidth unused.

4.2 Simulations

A total of 30 simulations are run: 2 demand scenarios, 5 different RA strategies and 3 executions for each case. On a computer with 7 cores, around 4 minutes per generation are needed. The strategies are:

- Allocate power but not bandwidth. This is what [14] implements. Each beam receives different values of power but all of them use 50% of the total satellite bandwidth.

- Allocate bandwidth but not power. Each beam receives P_{tot}/N watts of power and different values of bandwidth (from 0% to 100% the total satellite bandwidth).

- Allocate power and bandwidth but limiting the possible bandwidths for each beam to:

  - 30% to 70% of the total satellite bandwidth

  - 20% to 80% of the total satellite bandwidth

  - 0% to 100% of the total satellite bandwidth (therefore, there are no restrictions)

4.2.1 Demand 1: moderate variation

The demand for this case is generated randomly imitating the range and mean of the demand used in [14]. The total data rate requested by the users under the 37 beams is 169.31 Gbps.

The results are shown on Table 4.3. "P" stands for power, "BW" for bandwidth and "gen" for generations. The best execution and average results are colored in green.

Table 4.3: Results of the genetic algorithm for the demand 1

Strategy	USC (Gbps)	MSC (Gbps)	P (W)	# gen
Uniform P and BW allocation	**19.45**	**149.86**	**2350**	**-**
P allocation but uniform BW				
Execution 1	9.61	159.7	2350	24
Execution 2	10.01	159.3	2334.8	19
Execution 3	9.53	159.78	2350	27
	9.72	**159.59**	**2344.9**	**23.3**
BW allocation (0% - 100%) but uniform P				
Execution 1	16.17	153.14	2350	17
Execution 2	16.17	153.14	2350	17
Execution 3	16.1	153.21	2350	15
	16.15	**153.16**	**2350**	**16.3**
P and BW allocation (30% - 70%)				
Execution 1	9.4	159.91	2318.3	19
Execution 2	8.43	160.88	2343.4	29
Execution 3	8.42	160.89	2350	23
	8.75	**160.56**	**2337.2**	**23.7**
P and BW allocation (20% - 80%)				
Execution 1	9.09	160.22	2350	25
Execution 2	8.69	160.62	2350	27
Execution 3	8.63	160.68	2350	35
	8.80	**160.51**	**2350**	**29**
P and BW allocation (0% - 100%)				
Execution 1	9.32	159.99	2340.9	26
Execution 2	8.83	160.48	2342.1	31
Execution 3	10.29	159.02	2350	26
	9.48	**159.83**	**2344.3**	**27.7**

As it can be observed, allocating only bandwidth is not a satisfactory strategy. If just one parameter had to be allocated, power would be a better choice (and thus this is the approach taken in much literature). The joint optimization of power and bandwidth that yields the best average results is the 30% - 70% case, probably because the demand does not have much variation and this limitation helps the algorithm (except for the first execution). For the 20% - 80% case the results are not as good on average, and they are even worse in the 0% - 100% case. Nevertheless, the difference between the 30% - 70% and the 20% - 80% case is smaller than the difference between executions, so both cases are considered similar. On average, the improvement on the USC of the power allocation with respect to the uniform power and bandwidth allocation is **50.04%** (54.27% in [14]). The improvement of allocating bandwidth as well with respect to just power is, for the 30-70 case, **9.95%**, which represents an extra decrease of 5% for the USC obtained in the uniform power and bandwidth case.

The following results are obtained from the best execution: the third one of the 30% - 70% cases.

In Figures 4-4 and 4-5, the algorithm's convergence is depicted. These figures show the maximum, average and minimum values of USC among the population. The algorithm stops after 23 generations, although perfect convergence is not achieved (which can be especially noticed in Figure 4-5).

Figure 4-6 shows the data rate obtained with the genetic algorithm, the data rate obtained with a uniform power and bandwidth allocation, and the demands in blue, white and red respectively. If a beam's power is 90% or more of P_b^{max}, a black dot is drawn above the blue data rate bar. It can be observed how the data rate bars follow the demand bars up to a certain point (when their power is P_b^{max}). The white bars would all be equal if there was no interference or atmospheric attenuation, two factors that make links different even with the same allocation of resources. As for the bandwidth, it is shown with squares under the bars colored proportionally. It can be observed that it is indeed traded between adjacent beams: for example, beams 1 and 3 have more than the average value of bandwidth (thus they are colored in blue) and, on the other hand, beam 2 has a lower bandwidth (and is colored in red).
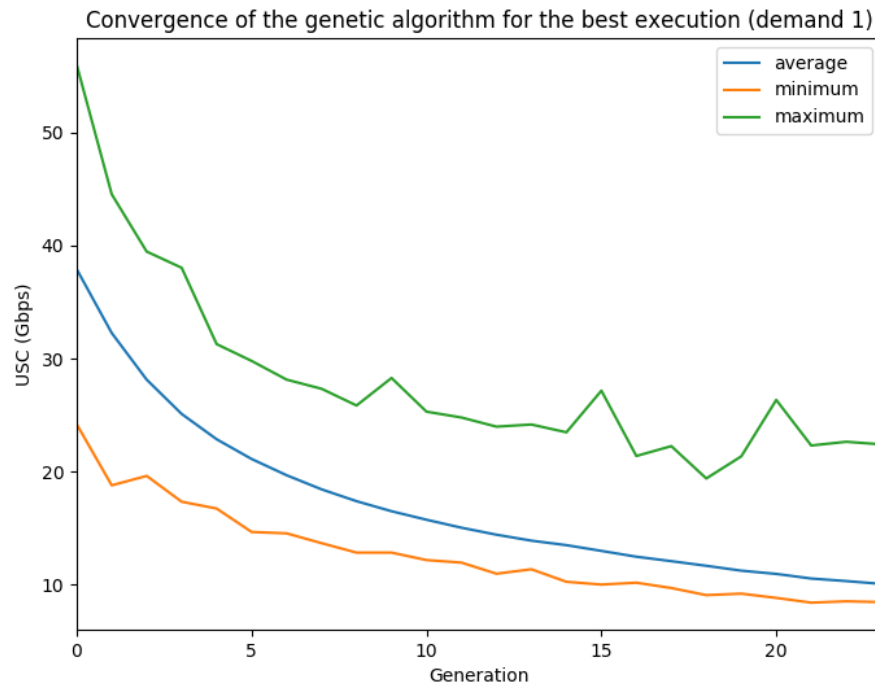
Figure 4-4: Convergence for the best execution of demand 1
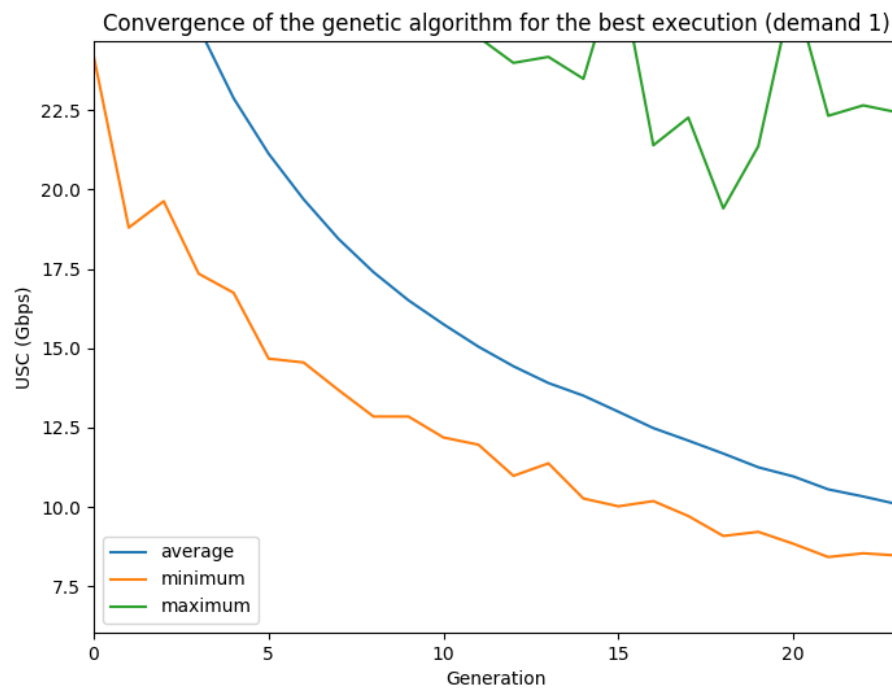

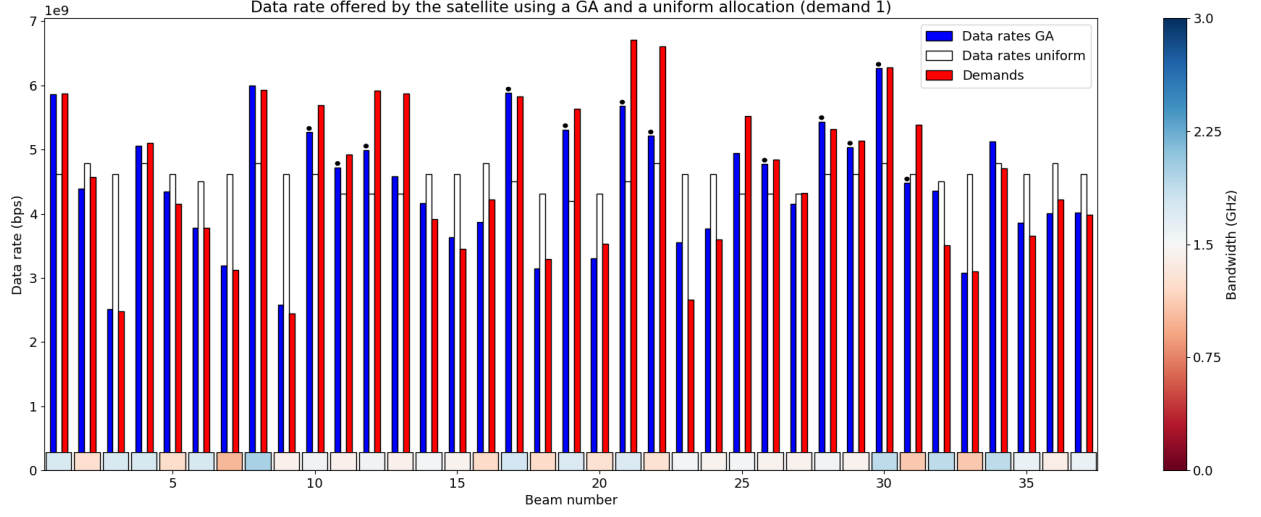Figure 4-5: Zoomed convergence for the best execution of demand 1

Figure 4-6: Data rates for the best execution of demand 1

Figure 4-7 presents an histogram of the bandwidths assigned to beams. 18 of them have less than 1.5 GHz (half the total satellite bandwidth), and 19 of them have more than 1.5 GHz. A small amount of bandwidth is "won": in the uniform bandwidth allocation case, the total bandwidth is $1.5 \cdot 37 = 55.5$ GHz, whereas in the dynamic bandwidth allocation case, the total bandwidth assigned to all 37 beams is 56.10 GHz. This may not seem intuitive, but Figure 4-8 shows an example that demonstrates how this can happen. The sum of the top 3 beams' bandwidth (whose number indicates their color) is 4.7 instead of $1.5 \cdot 3 = 4.5$. That is, 0.2 GHz of bandwidth is "won".

This phenomenon causes the algorithm to give more bandwidth to beams that are on the sides. Thus, colors 0 and 3, which have more exterior beams, have an average bandwidth per beam of 1.54 GHz and 1.83 GHz respectively, higher than colors 1 and 2 with just 1.18 GHz and 1.47 GHz.

Nevertheless, the algorithm might also leave some bandwidth unused: a beam might be limited in bandwidth by the one to the left but have a "gap" with the one to the right, shown on the second row from the bottom in Figure 4-8. The total sum of bandwidth "unused" is 0.44 GHz.
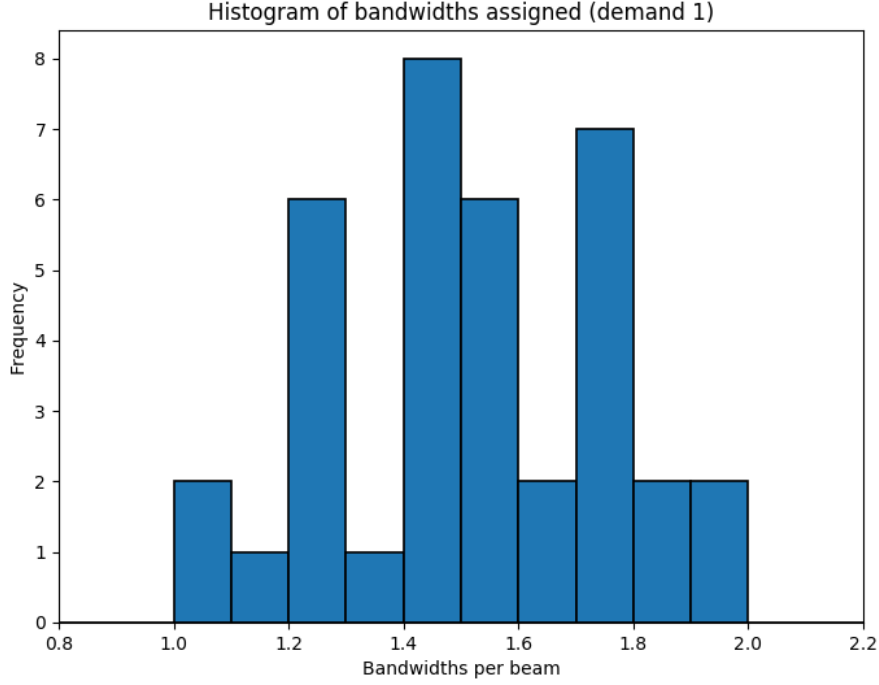
Figure 4-7: Bandwidths' histogram for the best execution of demand 1

4.2.2 Demand 2: high variation

Demand 2 has the same average than demand 1, but values' range is from 0 to the double of the previous ones. The total data rate requested by the users under the beams is 172.07 Gbps.

The results are shown on Table 4.4. Again, the best execution and average results are colored in green.

As in the previous case, it can be observed that allocating only bandwidth yields weak results. In this case, the joint optimization of power and bandwidth that produces the best average results is the 0% - 100% case, probably because the demand has more variation and more freedom can provide some executions to yield better results. Nevertheless, this flexibility also causes poor performances such as in execution 3. The results obtained for the 30% - 70% and 20% - 80% cases are similar. On average, the improvement of the power allocation with respect to the uniform power and bandwidth allocation is **22.03%**. The improvement of allocating bandwidth as
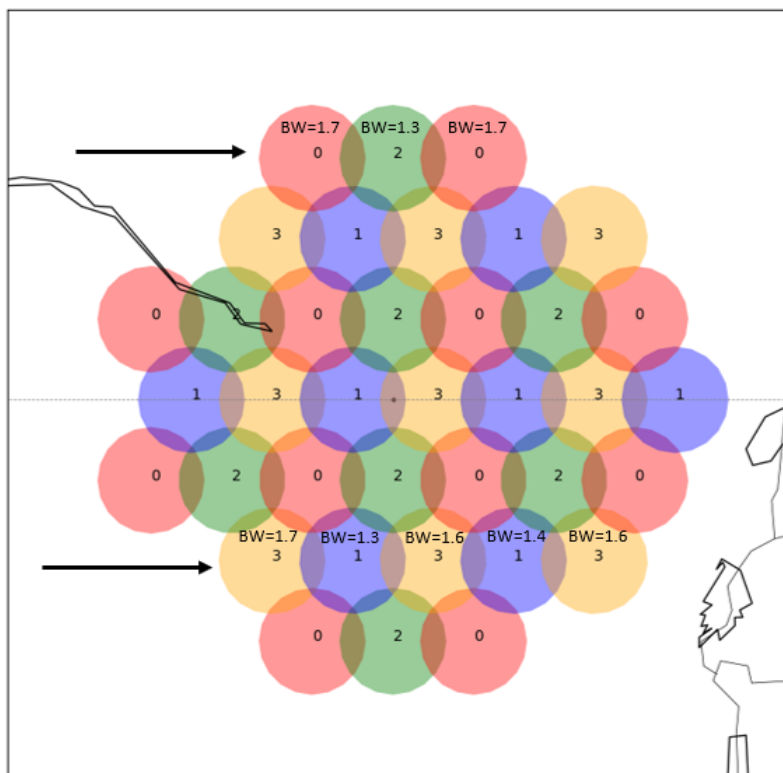
60

Figure 4-8: Examples of scenarios where bandwidth is "won" (which happens in the upper row indicated with an arrow) and "unused" (which happens in the lower row indicated with an arrow)

Table 4.4: Results of the genetic algorithm for the demand 2

Strategy	USC (Gbps)	MSC (Gbps)	P (W)	# gen
Uniform P and BW allocation	**40.88**	**131.19**	**2350**	**-**
P allocation but uniform BW				
Execution 1	31.96	140.11	2211.1	15
Execution 2	31.7	140.37	2270.6	15
Execution 3	31.96	140.11	2350	15
	31.87	**140.20**	**2277.2**	**15**
BW allocation (0% - 100%) but uniform P				
Execution 1	35.36	136.71	2350	15
Execution 2	35.34	136.73	2350	15
Execution 3	35.34	136.73	2350	15
	35.35	**136.72**	**2350**	**15**
P and BW allocation (30% - 70%)				
Execution 1	26.92	145.15	2201.6	21
Execution 2	27.2	144.87	2244.3	19
Execution 3	28.04	144.03	2305.1	17
	27.39	**144.68**	**2250.3**	**19**
P and BW allocation (20% - 80%)				
Execution 1	27.96	144.11	2350	15
Execution 2	26.39	145.68	2319.4	22
Execution 3	27.97	144.1	2330.2	15
	27.44	**144.63**	**2333.2**	**17.3**
P and BW allocation (0% - 100%)				
Execution 1	26.04	146.03	2339.6	25
Execution 2	27.02	145.05	2350	20
Execution 3	28.76	143.31	2278.9	16
	27.27	**144.80**	**2322.8**	**20.3**

well with respect to just power is, for the 0-100 case, **14.43%**, which represents an extra decrease of 11% in the USC with respect to the uniform power and bandwidth allocation. This increase is higher than the obtained in demand 1, as expected: a more variated demand is in more need of a joint power and bandwidth allocation. Apart from allocating more power, the data rate requested in the beams with high demands can be supplied by giving more bandwidth to those beams while reducing

it in the beams with low demands.

The following results are obtained from the best execution: the first one of the 0% - 100% cases.

In Figures 4-9 and 4-10, the algorithm's convergence is depicted. It is achieved after 25 generations.

Figure 4-11 shows the data rates obtained together with the demands. In this case, the blue bars reach higher data rates because bandwidth allocation is completely flexible. While in the best case for demand 1 the maximum data rate was approximately 6.5 Gbps, in this case the first beam provides about 8 Gbps. This beam is allocated most of the available bandwidth and, of course, the adjacent beam has virtually no bandwidth assigned.

The histogram of bandwidths assigned to beams is shown in Figure 4-12. Again, 18 beams have less than 1.5 GHz (half the total satellite bandwidth) and 19 of them have more than 1.5 GHz, but a much higher variance can be observed. The total bandwidth is 56.64 GHz instead of the 55.5 GHz that a uniform allocation would yield. Due to the increased flexibility in bandwidth allocation in comparison with the previous demand scenario, the amount of GHz "won" is higher.

As in the case of demand 1, the algorithm gives more bandwidth to beams that are on the sides; colors 0 and 3 have an average bandwidth per beam of 1.73 GHz and 1.55 GHz respectively, higher than in colors 1 and 2 with just 1.44 GHz and 1.30 GHz. The total sum of bandwidth "unused" is, in this case, 2.43 GHz, a much greater value than in the previous demand scenario.
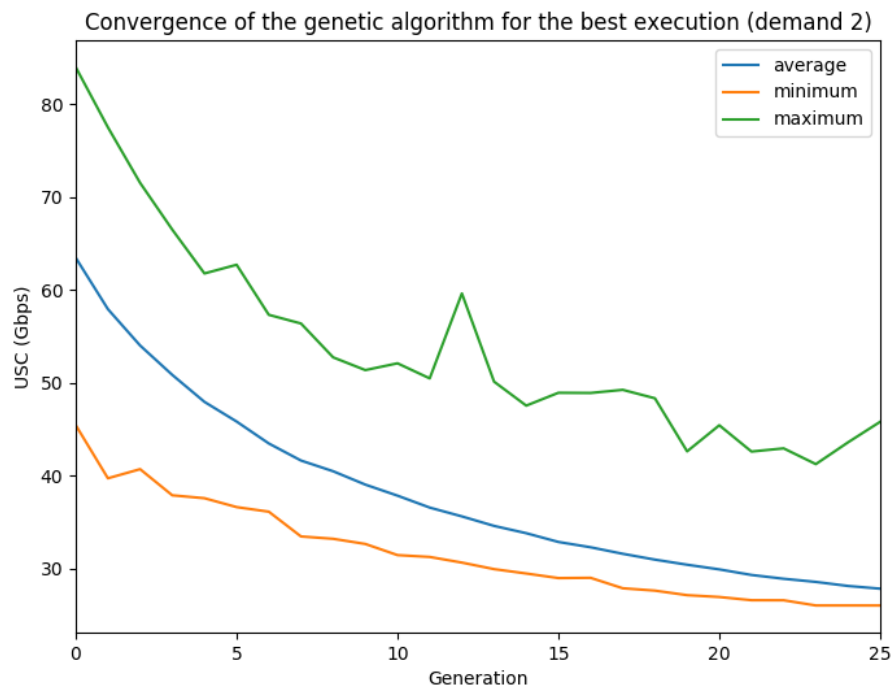
Figure 4-9: Convergence for the best execution of demand 2

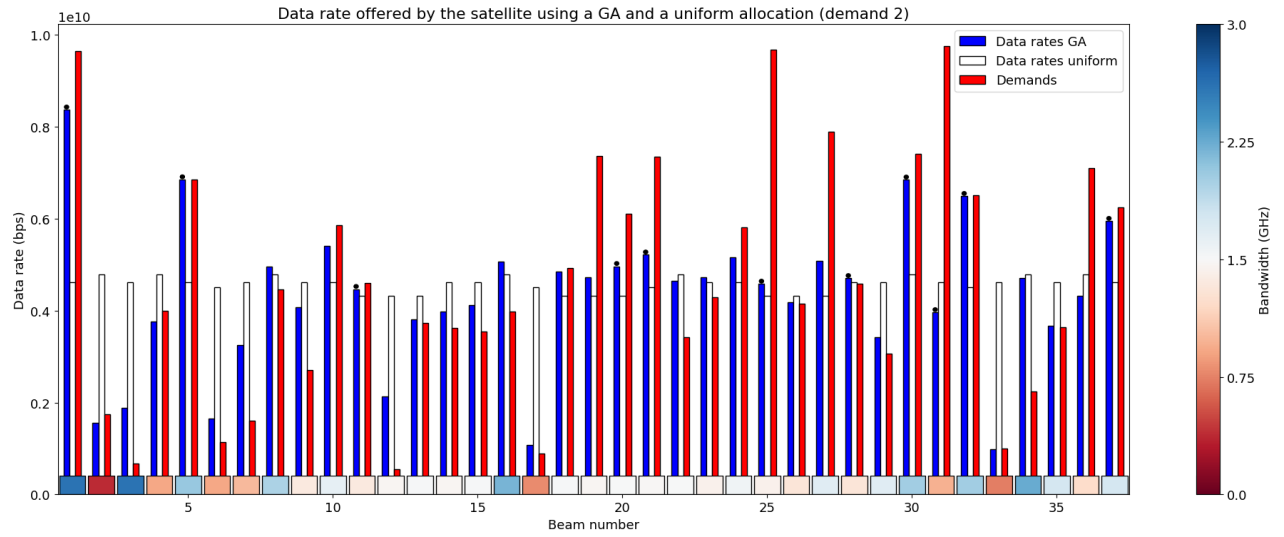Figure 4-10: Zoomed convergence for the best execution of demand 2

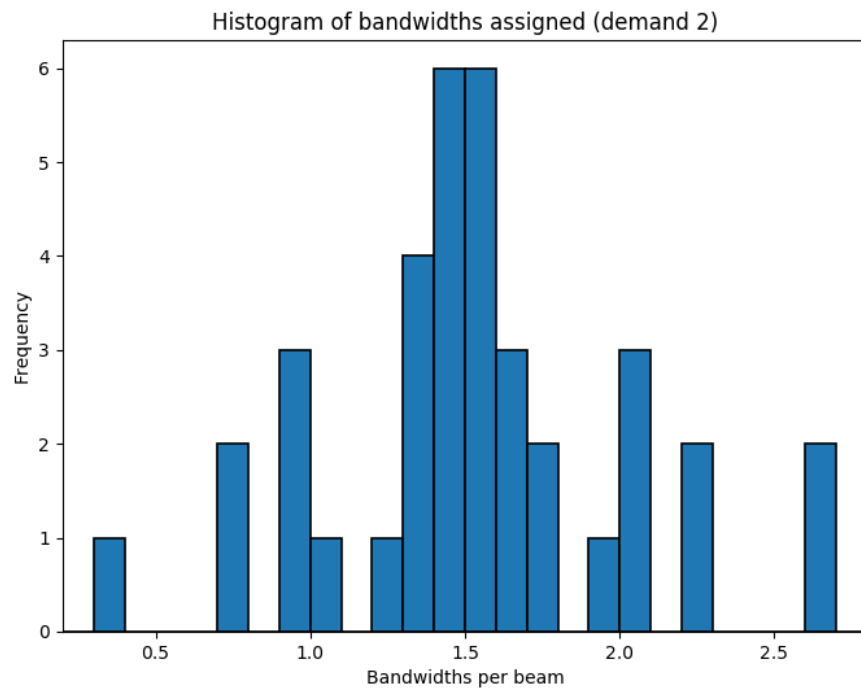Figure 4-11: Data rates for the best execution of demand 2

Figure 4-12: Bandwidth's histogram for the best execution of demand 2

Chapter 5

Conclusions

This chapter summarizes the main points of this thesis in Section 5.1. The main findings are exposed in Section 5.2 and, finally, Section 5.3 outlines opportunities for future research on this topic.

5.1 Summary

This thesis analyzes the problem of power and bandwidth allocation in multibeam communications satellites subject to interferences and atmospheric attenuation. Chapter 1 studies the literature and finds the research gap that motivates this thesis: a lack of metaheuristics/artificial intelligence algorithms that allocate both power and bandwidth while considering aspects such as interferences between beams.

Chapter 2 outlines the fundamentals of satellite communications theory, presents the system model and analyzes simple case studies. As shown, the optimal strategy is to allocate power and bandwidth in a proportional manner, but the system presents nonlinearities (the optimal points, although close, are not in the diagonal of the power and bandwidth diagram).

Chapter 3 states the problem this thesis solves and defines the proposed solution to it: a genetic algorithm that allocates power and bandwidth subject to several constraints for these resources.

Finally, the results obtained by performing simulations on the problem are shown

in Chapter 4. These results reveal that the USC can be reduced in 10% - 15% by allocating power and bandwidth compared to a power-only allocation, and that when the variation of the demand is increased, the optimal strategy is to allow bandwidths a higher flexibility.

5.2   Main findings

Power and bandwidth have an important effect on the data rate provided by a communications satellite. Thus, this thesis has studied their influence in the performance with simple problems and has expanded the approach taken in [14] to bandwidth allocation. The main conclusions are:

- The best performance is achieved when power and bandwidth are allocated in a proportional manner (that is, when a similar percentage of both resources is given to a beam: the optimal points are around the diagonal in the power and bandwidth diagrams). Nevertheless, there are nonlinearities in the MODCODs and this phenomenon caused optimal points to be slightly outside the diagonal in the cases studied in Section 2.3.

- Apart from allocating power, the unmet system capacity can be further reduced by allocating bandwidths per beam.

- The approach taken in Section 3.2 to allocate both resources can diminish the USC in 10% - 15% compared to a power-only allocation.

- The spatial variability of the demand has an effect on that improvement: the higher it is, the more important it is to allocate also bandwidths, as well as to allow the genetic algorithm a higher flexibility to allocate these bandwidths in order to obtain the best solution (and vice versa). While it is true this flexibility does not yield a significant improvement on average, specific executions have the potential to minimize in more extent the USC.

5.3   Future work

As previously exposed, this thesis has made several assumptions to simplify the problem. Therefore, a more detailed and complex system could be analyzed in the future, and several other approaches may be taken. Possible extensions of this thesis may cover:

- With the advent of phased array antennas, beams will need to be pointed and their size be chosen depending on the demand (beamforming), which is an NP-hard problem as well.

- The proposed solution to the problem this thesis approaches uses a genetic algorithm. Recently, there have been advancements on artificial intelligence and especially machine learning. Therefore, applying these techniques to improve the resource allocation is suggested.

- The interference model is explained in Chapter 2. Future research could implement a higher fidelity one that, for example:

  - Determines the carrier to interference ratio due to third order modulation products (C3IM) using the specific curve for each MODCOD instead of one curve for all MODCODs.

  - Determines the carrier to adjacent beam interference ratio (CABI) at the beam footprint edges, where it is lower than in the center (there is more interference).

- Instead of only performing a link budget calculation on the beam footprint center, it could be done on the beam footprint edge, to be conservative.

- An analysis of how the algorithm scales with the number of beams (and colors) would be useful since future communications satellites will have high numbers of them.

- For similar reasons, the algorithm efficiency may be improved.

- A sensitivity analysis over the demand should be performed, with different scenarios and more experiments per demand model.

- Last but not least, it is suggested to more accurately reproduce the system model of [14] so results can be compared with more certainty.

Bibliography

[1] SES S.A. New frontiers annual report 2017, 2017.

[2] Gérard Maral and Michel Bousquet. *Satellite communications systems: systems, techniques and technology.* John Wiley & Sons, 2011.

[3] William W Wu. Satellite communications. *Proceedings of the IEEE*, 85(6):998–1010, 1997.

[4] Cédric Balty, Jean-Didier Gayrard, and Patrick Agnieray. Communication satellites to enter a new age of flexibility. *Acta Astronautica*, 65(1-2):75–81, 2009.

[5] David Whitefield and Rajeev Gopal. Capacity enhancement with dynamic resource management for next generation satellite systems. In *Military Communications Conference, 2005. MILCOM 2005. IEEE*, pages 761–767. IEEE, 2005.

[6] John J Knab. Optimization of commercial satellite transponders and terminals. *IEEE Transactions on Aerospace and Electronic Systems*, 49(1):617–622, 2013.

[7] Piero Angeletti, David Fernandez Prim, and Rita Rinaldo. Beam hopping in multi-beam broadband satellite systems: System performance and payload architecture analysis. In *24th AIAA International Communications Satellite Systems Conference*, page 5376, 2006.

[8] J Anzalchi, A Couchman, C Topping, P Gabellini, G Gallinaro, L D'Agristina, P Angeletti, N Alagha, and A Vernucci. Beam hopping in multi-beam broadband satellite systems. 2009.

[9] J Anzalchi, A Couchman, P Gabellini, G Gallinaro, L D'agristina, N Alagha, and P Angeletti. Beam hopping in multi-beam broadband satellite systems: System simulation and performance comparison with non-hopped systems. In *Advanced satellite multimedia systems conference (ASMA) and the 11th signal processing for space communications workshop (SPSC), 2010 5th*, pages 248–255. IEEE, 2010.

[10] Shree Krishna Sharma, Sina Maleki, Symeon Chatzinotas, Joel Grotz, Jens Krause, and Björn Ottersten. Joint carrier allocation and beamforming for cognitive satcoms in ka-band (17.3–18.1 ghz). In *Communications (ICC), 2015 IEEE International Conference on*, pages 873–878. IEEE, 2015.

[11] Shree Krishna Sharma, Eva Lagunas, Sina Maleki, Symeon Chatzinotas, Joel Grotz, Jens Krause, and Björn Ottersten. Resource allocation for cognitive satellite communications in ka-band (17.7–19.7 ghz). In *Communication Workshop (ICCW), 2015 IEEE International Conference on*, pages 1646–1651. IEEE, 2015.

[12] Eva Lagunas, Shree Krishna Sharma, Sina Maleki, Symeon Chatzinotas, and Björn Ottersten. Resource allocation for cognitive satellite communications with incumbent terrestrial networks. *IEEE Transactions on Cognitive Communications and Networking*, 1(3):305–317, 2015.

[13] Barry D Van Veen and Kevin M Buckley. Beamforming: A versatile approach to spatial filtering. *IEEE assp magazine*, 5(2):4–24, 1988.

[14] Alexis I Aravanis, Bhavani Shankar MR, Pantelis-Daniel Arapoglou, Grégoire Danoy, Panayotis G Cottis, and Björn Ottersten. Power allocation in multibeam satellite systems: A two-stage multi-objective optimization. *IEEE Transactions on Wireless Communications*, 14(6):3171–3182, 2015.

[15] Jiang Lei and Maria Angeles Vazquez-Castro. Joint power and carrier allocation for the multibeam satellite downlink with individual sinr constraints. In *Communications (ICC), 2010 IEEE International Conference on*, pages 1–5. IEEE, 2010.

[16] Martin Schubert, Holger Boche, et al. Qos-based resource allocation and transceiver optimization. *Foundations and Trends® in Communications and Information Theory*, 2(6):383–529, 2006.

[17] Zhe Ji, Youzheng Wang, Wei Feng, and Jianhua Lu. Delay-aware power and bandwidth allocation for multiuser satellite downlinks. *IEEE Communications Letters*, 18(11):1951–1954, 2014.

[18] YuanZhi He, YiZhen Jia, and XuDong Zhong. A traffic-awareness dynamic resource allocation scheme based on multi-objective optimization in multi-beam mobile satellite communication systems. *International Journal of Distributed Sensor Networks*, 13(8):1550147717723554, 2017.

[19] Haitao Wang, Zhihui Liu, Zijing Cheng, Ye Miao, Wei Feng, and Ning Ge. Maximization of link capacity by joint power and spectrum allocation for smart satellite transponder. In *Communications (APCC), 2017 23rd Asia-Pacific Conference on*, pages 1–6. IEEE, 2017.

[20] Heng Wang, Aijun Liu, and Xiaofei Pan. Optimization of joint power and bandwidth allocation in multi-spot-beam satellite communication systems. *Mathematical Problems in engineering*, 2014, 2014.

[21] Digital Video Broadcasting (DVB). Implementation guidelines for the second generation system for broadcasting, interactive services, news gathering and other broadband satellite applications; Part 2 - S2 extensions (DVB-S2X), 2015.

[22] International Telecommunication Union Radiocommunication Sector (ITU-R). Recommendation ITU-R S.1528: Satellite antenna radiation patterns for non-geostationary orbit satellite antennas operating in the fixed-satellite service below 30 GHz, 2001.

[23] Athanasios D Panagopoulos, Pantelis-Daniel M Arapoglou, and Panayotis G Cottis. Satellite communications at Ku, Ka, and V bands: Propagation impairments and mitigation techniques. *IEEE Communications Surveys & Tutorials*, 6(3), 2004.

[24] International Telecommunication Union Radiocommunication Sector (ITU-R). Recommendation ITU-R P.618-12: Propagation data and prediction methods required for the design of earth-space telecommunication systems, 2015.

[25] International Telecommunication Union Radiocommunication Sector (ITU-R). Recommendation ITU-R P.676-11: Attenuation by atmospheric gases, 2016.

[26] International Telecommunication Union Radiocommunication Sector (ITU-R). Recommendation ITU-R P.840-6: Attenuation due to clouds and fog, 2013.

[27] Alexis I Aravanis, Gregoire Danoy, Pantelis Arapoglou, Panayotis G Cottis, and Björn Ottersten. Multi-objective optimization approach to power allocation in multibeam systems. In *30th AIAA International Communications Satellite System Conference (ICSSC)*, page 15202, 2012.

[28] Jan van Leeuwen. *Handbook of Theoretical Computer Science. Vol. A, Algorithms and Complexity*. MIT Press/Elsevier Science Publishers, 1998.

[29] Scott Aaronson. Guest column: NP-complete problems and physical reality. *ACM Sigact News*, 36(1):30–52, 2005.

[30] Melanie Mitchell. *An introduction to genetic algorithms*. MIT Press, 1998.

[31] Félix-Antoine Fortin, François-Michel De Rainville, Marc-André Gardner, Marc Parizeau, and Christian Gagné. DEAP: Evolutionary algorithms made easy. *Journal of Machine Learning Research*, 13:2171–2175, jul 2012.

[32] Yannick Hold-Geoffroy, Olivier Gagnon, and Marc Parizeau. Once you scoop, no need to fork. In *Proceedings of the 2014 Annual Conference on Extreme Science and Engineering Discovery Environment*, page 60. ACM, 2014.

[33] BGW Craenen, AE Eiben, and E Marchiori. How to handle constraints with evolutionary algorithms. *Practical Handbook Of Genetic Algorithms: Applications*, pages 341–361, 2001.